



Provided by the author(s) and University College Dublin Library in accordance with publisher policies., Please cite the published version when available.

Title	Non-viral gene delivery by minicircle vector expressing type VII collagen for the treatment of recessive dystrophic epidermolysis bullosa
Authors(s)	Qin, Yue
Publication date	2017
Publisher	University College Dublin. School of Medicine
Link to online version	http://dissertations.umi.com/ucd:10154
Item record/more information	http://hdl.handle.net/10197/8668

Downloaded 2018-08-17T10:52:08Z

The UCD community has made this article openly available. Please share how this access benefits you. Your story matters! (@ucd_oa)



Some rights reserved. For more information, please see the item record link above.





Non-viral Gene Delivery by Minicircle Vector Expressing Type VII Collagen for the Treatment of Recessive Dystrophic Epidermolysis Bullosa

Yue Qin, B.Eng.

UCD Student No.: 14206761

The thesis is submitted to University College Dublin
in fulfilment of the requirements for the degree of

Master of Science (Research)

Charles Institute of Dermatology

School of Medicine

Head of School: Prof. Patrick Murray

Principal Supervisor: Prof. Wenxin Wang

Members of the Research Masters Panel:

Prof. Sabine Koelle

Prof. Martin Steinhoff

Prof. Frank Powell

January 2017

Table of Contents

TABLE OF CONTENTS	I
LIST OF FIGURES AND TABLES	III
ABSTRACT	IV
STATEMENT OF ORIGINAL AUTHORSHIP	V
ACKNOWLEDGEMENTS	VI
LIST OF ABBREVIATIONS	VII
CHAPTER ONE	1
INTRODUCTION	1
1.1 BACKGROUND	1
1.1.1 <i>Recessive Dystrophic Epidermolysis Bullosa</i>	1
1.1.2 <i>Current Research Directions Towards RDEB Therapy</i>	3
1.1.3 <i>Current Ongoing Clinical Trials for EB</i>	9
1.1.4 <i>Minicircle Gene Therapy for RDEB</i>	14
1.2 HYPOTHESES AND OBJECTIVES	19
CHAPTER TWO	21
MATERIALS AND METHODS	21
2.1 MATERIALS.....	21
2.2 METHODS	21
2.2.1 <i>Minicircle Amplification and Purification</i>	21
2.2.2 <i>Construction of Minicircle Vector with COL7A1 Expression Gene</i>	22
2.2.3 <i>Cell Cultures</i>	22
2.2.4 <i>Cell Transfection</i>	22
2.2.5 <i>Fluorescence Detection and Flow Cytometry</i>	22
2.2.6 <i>Western Blotting</i>	23
CHAPTER THREE	24
RESULTS AND DISCUSSION	24
3.1 MINICIRCLE DNA PRODUCTION AND CHARACTERISATION	24
3.1.1 <i>Production of Minicircle Vector with Reporter Gene</i>	24
3.1.2 <i>Optimisation of Minicircle Delivery Methodology</i>	26
3.1.3 <i>Evaluation of Long-Term Gene Expression on MC and PP Vectors</i>	30
3.2 RESTORATION OF TYPE VII COLLAGEN <i>IN VITRO</i>	36
3.2.1 <i>Construction of Minicircle-COL7A1 and Parental Plasmid-COL7A1</i>	37
3.2.2 <i>Effect of Minicircle on Long-Term Expression of Type VII Collagen</i>	40

CHAPTER FOUR	43
CONCLUSIONS AND FUTURE DIRECTIONS	43
4.1 CONCLUSIONS.....	43
4.2 FUTURE DIRECTIONS	43
REFERENCES	45
APPENDIX I	55
CONSTRUCTION OF MINICIRCLE-COL7A1 WITH TISSUE-SPECIFIC PROMOTER	55
APPENDIX II	61
MATERIALS AND PROTOCOLS	61

List of Figures and Tables

FIGURE 1 STATISTICS OF DIFFERENT THERAPIES ON CLINICAL TRIALS RELATED TO EB.....	9
FIGURE 2 A SCHEMATIC REPRESENTATION OF A GENERIC THERAPEUTIC PLASMID DNA VECTOR.	15
FIGURE 3 SCHEMATIC REPRESENTATION OF MINICIRCLE VECTORS.	17
FIGURE 4 MINICIRCLE PRODUCTION PROCEDURES.....	21
FIGURE 5 SCHEMATIC REPRESENTATION OF Φ C31 RECOMBINASE/I-SCE I ENDONUCLEASE MINICIRCLE SYSTEM VECTOR.	25
FIGURE 6 DNA ELECTROPHORESIS OF THE PP AND MC VECTOR.	26
FIGURE 7 EVALUATION OF THE TRANSFECTION EFFICIENCY OF THE MC AND PP VECTORS WITH GFP REPORTER IN HELA CELLS VIA LIPOFECTAMINE® 2000 REAGENT.	27
FIGURE 8 EVALUATION OF THE TRANSFECTION EFFICIENCY OF THE MC AND PP VECTORS WITH GFP REPORTER IN 3T3 CELLS VIA LIPOFECTAMINE® 2000 REAGENT.	28
FIGURE 9 EVALUATION OF THE TRANSFECTION EFFICIENCY OF THE MC AND PP VECTORS WITH GFP REPORTER IN HELA CELLS VIA XFECT™ REAGENT.....	29
FIGURE 10 EVALUATION OF THE TRANSFECTION EFFICIENCY OF THE MC AND PP VECTORS WITH GFP REPORTER IN 3T3 CELLS VIA XFECT™ REAGENT.	30
FIGURE 11 TRANSFECTION ASSESSMENT OF THE MC AND PP VECTORS IN HELA CELLS TWO DAYS POST TRANSFECTION.	33
FIGURE 12 TRANSFECTION ASSESSMENT OF THE MC AND PP VECTORS IN NHK CELLS TWO DAYS POST TRANSFECTION.	34
FIGURE 13 TRANSFECTION ASSESSMENT OF THE MC AND PP VECTORS IN RDEBK CELLS TWO DAYS POST TRANSFECTION.	35
FIGURE 14 FLOW CYTOMETRY ANALYSIS OF TRANSFECTED GFP POSITIVE CELLS BY THE PP AND MC VECTORS UP TO TWO WEEKS.....	36
FIGURE 15 SCHEMATIC DIAGRAM OF (A) PARENTAL PLASMID-COL7A1 (PP-COL7A1), (B) MINICIRCLE-COL7A1 (MC-COL7A1) AND (C) pCDNA3.1/COL7A1 VECTOR.....	38
FIGURE 16 CHARACTERISATION OF THE PARENTAL PLASMID-COL7A1 (PP-COL7A1) AND MINICIRCLE-COL7A1 (MC-COL7A1) STRUCTURE.	39
FIGURE 17 REPRESENTATIVE IMAGES OF RED FLUORESCENCE EXPRESSION ON TRANSFECTED RDEB KERATINOCYTES (RDEBK) UP TO 15 DAYS POST MC-COL7A1 AND PP-COL7A1 TRANSFECTION.....	41
FIGURE 18 WESTERN BLOTTING RESULTS FOR CONCENTRATED SUPERNATANT HARVESTED ON 3 TO 15 DAYS POST TRANSFECTION.	42
TABLE 1 ONGOING CLINICAL TRIALS ON EB	10

Abstract

Recessive Dystrophic Epidermolysis Bullosa (RDEB) is a rare genetic skin disorder caused by mutations in the COL7A1 gene. The lack of type VII collagen results in absent anchoring fibrils which may cause the separation of the epidermis from the dermis in response to minimal trauma or friction. RDEB patients suffer from severe blistering and chronic wounds with their lifetimes. Unfortunately, there is no effective treatment for RDEB to date. Among all the currently investigating methods, gene therapy directly correct COL7A1 gene expression in the targeted cells. Compared to viral gene vector, the non-viral vector is a realistic alternative that increases gene cargo capability and decreases the safety risks. However, the bacterial backbone on the non-viral vector and the relatively large size of COL7A1 limits its transfection efficiency and the protein restoration. Here, an efficient non-viral minicircle vector was investigated by removing the bacterial backbone which includes prokaryote origin and antibiotic resistance gene. The reduced vector size can significantly increase the transfection efficiency. In addition, the silencing effect of the target gene can be decreased with lower immunoreactivity which leads to a long-term expression of type VII collagen. In this thesis, proper transfection approach was firstly selected from current commercially available reagents; then, the transfection efficiencies between minicircle and parental plasmid vectors were compared in different cell types. Minicircle vector with COL7A1 gene was constructed. Our preliminary results suggested that the minicircle-COL7A1 gene vector significantly increased the transfection efficiency and prolonged the expression of type VII collagen *in vitro*. To further improve the minicircle system, a tissue-specific promoter driving COL7A1 gene expression in *Homo sapiens* was introduced into the minicircle vector for future systemic delivery study. The minicircle system has shown promise as a potential RDEB gene therapy treatment.

Statement of Original Authorship

I hereby certify that the submitted work is my own work, was completed while registered as a candidate for the degree stated on the Title Page, and I have not obtained a degree elsewhere on the basis of the research presented in this submitted work.

Acknowledgements

I would like to sincerely thank Prof. Wenxin Wang for his guidance and support throughout this project. I would like to thank Prof. Xuejun Hu for his support in the field of molecular biology. I would like to acknowledge Science Foundation Ireland and School of Medicine in UCD for their financial support.

Thanks to all at Charles Institute of Dermatology, who have lent a helping hand. I would also like to specifically thank Dr. Jian-yuan Huang for his basic cell culture training and unselfish help; Dr. Lara Cutlar for her help in my beginning step; Mr. Yongsheng Gao for his timely care and help when I was sick; Mr. Martin Karl for his assistance on gene transfection; Ms. Fatma Alshehri for her help on experiments and her tender heart; Mr. Jonathan O’Keeffe-Ahern for his help on language editing of my literature draft; Dr. Alfonso Blanco at UCD Conway Flow Cytometry Core for his kind assistance on flow cytometry analysis; Dr. Udo Greiser and Dr. Ruth Foley for their assistance in laboratory managements; Dr. Dezhong Zhou, Mr. Sigen A, Dr. Hong Zhang, Dr. Tianyu Zhao for their help during my study. Many deep thanks to Dr. Yixiao Dong for his support in various aspects, helping me through ups and downs in these years. Finally, I would like to thank my parents for backing me up always.

List of Abbreviations

AAV	Adeno-associated Virus
AF	Anchoring Fibril
ARM	Antibiotic Resistance Marker
BM	Bone Marrow
BMZ	Basement Membrane Zone
C7	Type VII Collagen
CMV	Cytomegalovirus
DEB	Dystrophic Epidermolysis Bullosa
DEJ	Dermal-Epidermal Junction
EB	Epidermolysis Bullosa
EBS	Epidermolysis Bullosa Simplex
EF1 α	Elongation Factor-1 α
GFP	Green Fluorescent Protein
GOI	Gene of Interest
HCT	Hematopoietic Cell Transplantation
iPSC	induced Pluripotent Stem Cell
JEB	Junctional Epidermolysis Bullosa
MC	Minicircle
MP	Miniplasmid
MSC	Mesenchymal Stromal/Stem Cell
NHK	Normal Human Keratinocyte
PP	Parental Plasmid
RDEB	Recessive Dystrophic Epidermolysis Bullosa
RDEBK	Recessive Dystrophic Epidermolysis Bullosa Keratinocyte

RFP	Red Fluorescent Protein
SCC	Squamous Cell Carcinoma
SIN	Self-inactivating
SV40	Simian Virus 40
UbC	Ubiquitin C
UCB	Umbilical Cord Blood

Chapter One

Introduction

1.1 Background

1.1.1 Recessive Dystrophic Epidermolysis Bullosa

Epidermolysis bullosa (EB) is a group of rare inherited skin disorder caused by mutated gene(s) that encode the structural cutaneous components^{1,2}. There are approximately over 500, 000 people affected by EB in the worldwide, and the prevalence of EB in Ireland is about 1/18,000 (<https://debraireland.org>). The human skin includes two major layers: the outer layer of the epidermis and the inner layer of the dermis. Based on different blistering regions of the wounded skin, EB can be classified into EB simplex (EBS), junctional EB (JEB), dystrophic EB (DEB) and Kindler syndrome³. In EBS, the disruption of junction confines in the epidermis. In JEB, the splitting is in the mid junction lamina lucida within the basement membrane zone (BMZ). In DEB, cleavages occur within the uppermost dermis right beneath the lamina densa of the BMZ. Kindler syndrome was reclassified in 2008 which describes the subtypes that blistering occurs at multiple levels of the skin³⁻⁵. Different subtypes of EB are caused by respective mutated proteins, such as transglutaminase 5 for EBS, keratin 5 for JEB and type VII collagen for DEB³.

DEB is one of the major subtypes that occupies about 20% of the whole EB population, among which Recessive Dystrophic Epidermolysis Bullosa (RDEB) usually results in more severe wounds in clinics than Dominant Dystrophic Epidermolysis Bullosa (DDEB)^{3,6}. As an inherited monogenic disorder, RDEB has been identified due to the mutations in both alleles of human COL7A1 gene, leading to a reduction or absence

of functional type VII collagen (C7)⁵. The human COL7A1 gene is located in the short-arm of human chromosome 3 (3p21), comprises 32 kb of genomic DNA and contains 118 exons. The resultant mRNA is 8.9 kb, encoding a 2944-amino acid (VII) polypeptide that can polymerise to procollagen VII homotrimers. By forming antiparallel dimers, two procollagen VII homotrimers constitute a large C7 molecule². C7 molecules form a major anchoring fibrils (AFs) by folding up to a triple-helical structure, which provides the dermal-epidermal junction (DEJ) in human skin⁷⁻⁹. So far, over 800 different mutations of COL7A1 has been reported (COL7A1 gene variants database, <http://www.col7.info>). Different mutations in COL7A1 result in varying degrees of symptoms. Nonsense or frameshift mutations on both alleles lead to premature termination of C7 synthesis and absent AFs production¹⁰. Patients with these mutations exhibit severe blistering and non-healed wounds which can be classified as “RDEB, generalised severe” (or named as “RDEB, Hallopeau-Siemens”)³. In contrast, milder clinical performances caused by missense mutations are classified as “RDEB, generalised intermediate” subtype (or named as “RDEB, non-Hallopeau-Siemens”)^{3,10}. In these subtypes, full-length C7 polypeptides can be synthesised¹¹, but their irregularity may prevent the AF assumption and aggregation¹².

The deficiency of functional C7 leads to poor adherence between dermis and epidermis. With minor trauma or friction, it is easy to form blistering and erosions on cutaneous and mucosal surfaces, e.g. oral mucosa, oesophagus, gastrointestinal tract¹³, eventually developing to mutilating scars and contractures¹⁴. Patients with RDEB usually suffer from the symptoms at birth or shortly afterwards. The chronic and severe skin erosions also cumulate the risk of squamous cell carcinoma (SCC) with the increase of age¹⁵. The life expectancy of RDEB patients is only 30 years in severe subtypes and a median survival of 55 to 65 years in milder phenotypes¹⁶.

1.1.2 Current Research Directions Towards RDEB Therapy

To date, there is no cure for RDEB in clinics, and patients are managed with only supportive care aimed at palliative wound care, pain management and quality of life maintaining¹⁷. However, some preclinical and clinical studies are proceeding to develop efficient therapies for RDEB, including protein injection, cell-based therapy, and gene therapy.

1.1.2.1 Protein Therapy

To restore the functional C7 in RDEB patients, the first protein-based therapy was described in 2004¹⁸. The human recombinant C7 protein was harvested from RDEB fibroblasts that transduced with lentiviral vectors containing full-length cDNA of human type VII collagen. Purified C7 protein was injected intradermally into nude mice and human RDEB skin grafted mice. It was demonstrated that the recombinant protein could transfer from the dermis to the BMZ and to form human AF structures between dermis and epidermis. It was shown that skin blistering was reduced with the restoration of C7 over two months post a single injection¹⁸. Subsequent studies with C7 knockout mouse model (Col7a1^{-/-}) also showed the similar results¹⁹. 88% of the treated mice restored BMZ adherence and prolonged their survival up to seven months¹⁹. Intradermal injection approach is restricted by its limited affecting radius and is difficult to be used at the mucosa area such as oral cavity and oesophagus, where lesions commonly occur in RDEB patients. Therefore, Woodley et al. demonstrated a systemic delivery approach by vein injecting human recombinant C7 in an RDEB skin-graft murine model, which showed increased AF formation and reduced dermis-epidermis separation²⁰. However, the short half-life of C7 protein usually requires multiple painful injections to the patients, and the potential pathogenic effects may also restrict the clinical application of protein-based therapies²¹.

1.1.2.2 Cell-Based Therapy

• Fibroblast Therapy

In human skin, C7 is mainly secreted by keratinocytes and fibroblasts^{22,23}. Compared to keratinocytes, fibroblasts are more robust and have presented less growth arrest or differentiation, which have been widely studied for RDEB treatments²⁴. In 2008, Wong et al. reported a clinical trial of fibroblast-based cell therapy on five patients with RDEB²⁵. In this study, fibroblasts from healthy donors were intradermally injected to the patients. C7 generation and AFs formation were observed up to three months post injection, but with an abnormal morphology. A one-year following-up study was performed to one of the original patients, who showed increased COL7A1 gene expression up to three months and an enhanced C7 level at the DEJ region for about nine months²⁶. It was also found that the heparin binding-EGF-like growth factor (HB-EGF) might enhance the patient's self C7 protein expression with partial functionalities²⁶. A following study on 11 patients with RDEB confirmed accelerated healing of erosion within 28 days post intradermal injection of allogeneic fibroblasts²⁷.

Besides allogeneic fibroblasts, engineered autologous fibroblasts have also been used for C7 restoration. Ortiz-Urda et al. transfected C7-deficient fibroblasts from RDEB patients by Φ C31 integrase-encoding plasmid of COL7A1 gene²⁴. The overexpressed fibroblasts improved the C7 expression in RDEB skin over 16 weeks *via* intradermal injection in an athymic nude murine model²⁴. Woodley et al. used lentiviral vectors infecting mutant fibroblasts, which showed the similar effectivity of secreting and depositing C7 at DEJ compared with normal human fibroblasts²⁸. After that, the lentiviral-vector-infected fibroblasts were injected intravenously in athymic nude mice with or without full-thickness human skin grafting. It was demonstrated that the engineered cells could home to the wound area and maintained C7 production at the wound sites²⁹. However, injected fibroblast deposition was also observed in lungs of

some mice, which raised potential safety risks for clinical uses²⁹.

- *Bone Marrow-Based Stem Cell Therapy*

In the last few years, stem cells have attracted unique advantages due to their multipotency, self-renew capacity and ability to secrete pro-regenerative cytokines³⁰. Bone marrow-derived stem cells are the most studied cell type for the past decades which has been used for RDEB treatments. In 2008, Chino et al. reported that transferred bone marrow cells into the embryo circulation of Col7a1^{-/-} mice, which ameliorated skin blistering in neonatal animals and lengthened the lifetime of those mice to 17-19 days versus two days in non-treatment control group³¹. In another study, it was demonstrated that wild-type marrow-derived hematopoietic stem cells could home to the skin lesions in Col7a1^{-/-} mice after birth and ameliorate the skin blistering phenotype by restoring C7 and AFs³². In 2010, Wagner et al. reported the first clinical trial of allogeneic hematopoietic cell transplanting (HCT) on seven children with RDEB³³. Two participants died in this study. One died before transplantation, probably because of the cyclophosphamide cardiotoxicity from immune myeloablative chemotherapy, and the other one died after 183 days due to the graft rejection and infection. Though this clinical trial showed potentials in HCT therapy for EB, the high morbidity and significant mortality should be resolved³³. It has been considered to apply a reduced-intensity non-myeloablative preparation on recipients before bone marrow transplantation^{34,35}. Other directions of stem cells therapy for RDEB include enhancing the safety and efficacy of HCT by co-infusing mesenchymal stromal/stem cells (MSCs), improving the homing of donor cells into skin erosions, as well as developing patient-specific induced pluripotent stem cells (iPSCs)³⁶. Alexeev et al. reported that autologous MSCs transplantation into Col7a1^{-/-} mouse skin displayed 15% C7 restoration levels compared to the wild-type mice, which had shown significant effects on preventing skin blister and wounds³⁷. In 2010, the first pilot clinical trial of using bone marrow-derived MSCs (BM-MSCs) on RDEB patients was reported by

Conget and colleagues³⁸. Two patients with severe RDEB were treated with the intradermal injection of allogeneic BM-MSCs at wound sites which showed remarkable improvement in the chronic wound healing for four months³⁸. Recently, an early phase clinical trial was published with allogeneic MSCs administration on ten children with RDEB³⁹. After nine months, the interviews indicated the improved wound healing in all patients and reduced skin erythema for 4-6 months occurred in 9 out of 10 patients³⁹. Other stem cell sources such as umbilical cord blood-derived MSCs (UBC-MSCs) have attracted growing interest in the field due to their relatively simple preparation process, which may indicate a promising potential on RDEB treatment⁴⁰⁻⁴². Also, considerations about the high susceptibility to infection and the increased risk of cancer development in RDEB patients should be highlighted related to the stem cell based therapies⁴³.

- *Induced Pluripotent Stem Cells (iPSCs)*

Induced pluripotent stem cells (iPSCs) are generated from somatic cells with comparable plasticity to embryonic stem cells (ESCs) without using human embryos, thereby avoiding the ethical issues⁴⁴. This advanced technique allows us to obtain sufficient numbers of stem cells from patients and prevent the immune rejection problem from allogeneic donors^{44,45}. Tolar et al. successfully generated iPSCs from fibroblasts and keratinocytes taken from three RDEB patients⁴⁶. These iPSCs were able to be differentiated into both hematopoietic and non-hematopoietic lineages and showed similar C7 expression and skin structure with the iPSCs derived from healthy skin cells⁴⁶. Sebastiano et al. developed iPSCs from primary human RDEB fibroblasts and keratinocytes, followed by correction of COL7A1 mutations using adeno-associated viral vectors (AAV)⁴⁷. Then the corrected iPSCs were further differentiated into epidermal keratinocytes and formed an autologous grafting sheet for treating RDEB chronic wounds. Keratinocytes differentiated from corrected iPSCs showed similar morphology and over 90% similarity on gene expression compared to normal human keratinocytes (NHKs)⁴⁷. Wenzel et al. showed that iPSC-derived fibroblasts

prevented blistering over 18 weeks in a Col7a1 mutant mouse model⁴⁸. However, as a newly developed technique, the obvious drawbacks of iPSCs limited its clinical applications, including the complicated generation procedures, the hardness of controlling differentiated production, the epigenetic proneness, the potential of transcriptional aberrations and the risk of inducing cancers⁴⁹.

1.1.2.3 Gene Therapy

Gene therapy aims to introduce the exogenous gene into patients' cells as a molecular medicine, which is directly correcting or displacing a distorted gene and accomplishing its expression functions⁵⁰. Gene therapies have been used for many acquired and inherited genetic diseases, including cystic fibrosis⁵¹, cancer⁵², acquired immunodeficiency syndrome (AIDS)⁵³, cardiovascular diseases⁵⁴ and X-linked severe combined immune deficiency (X-linked SCID)⁵⁵. Thousands of clinical trials have been investigated.

The vectors used in gene therapy can be categorised into two types: viral vectors and non-viral vectors⁵⁶. The majority of the gene therapy studies are based on viral vectors because of the high transduction efficiency. The basic principle of viral gene therapy is to modify the viruses to keep their infectious ability and integrate the gene of interest into cell chromosomes to express target proteins. Different viruses have been studied for gene therapies such as retroviral vectors, lentiviral vectors, adenoviral vectors, adeno-associated viral vectors (AAVs) and herpes simplex virus⁵⁷. Besides their high efficiencies, the use of the viral vectors for RDEB treatment was significantly hampered by the large size of COL7A1 gene. To overcome this problem, Chen et al. developed a "minigene" of COL7A1 to produce "type VII minicollagen" to fit for retroviral-mediated vectors⁵⁸. The gene-corrected DEB keratinocytes could sustain the minicollagen expression for over eight months *in vitro*, with enhanced cell-substratum adhesion and decreased cell motility⁵⁸. A following study from the same group used a self-inactivating

(SIN) minimal lentivirus-based vector to express the full-length C7 in human RDEB keratinocytes and regenerate human skin on immune-deficient mice⁵⁹. The C7 expression was restored in gene-corrected RDEB cells, and AFs formation was promoted, which could be maintained *in vitro* for at least five months and about two months *in vivo*. They also modified the promoter from murine leukaemia virus driving the expression of C7 to reduce the circumvention of viral promoter methylation effect⁵⁹. Baldeschi et al. reported that a retrovirus-based vector transducing full-length canine-derived COL7A1 cDNA had improved the C7 restoration in both human and canine RDEB keratinocytes⁶⁰. Soon after, these retroviral vectors were utilised in the relatively longer human COL7A1 cDNA⁶¹. Transduced RDEB keratinocytes were grafted onto severe combined immunodeficiency (SCID) mice with the observation of skin structure restoration⁶¹. The application of SIN retroviral vectors was also developed for transducing primary keratinocytes and fibroblasts combined with human internal promoters⁶². It was indicated that over 60% transduced cells with internal promoters were detected to express C7 and the epidermal adherence was restored in the grafted skin⁶².

Although it has been shown some success on C7 restoration by viral vectors, their carcinogenesis risk and high immune responses hamper the clinical applications of these treatment approaches. On the contrary, non-viral vectors inhibit the potential biosafety risk, cytotoxicity and can transfer larger size gene⁵⁶. For example, plasmid vectors are less restricted by gene cargo size. It has been reported to deliver full-length COL7A1 cDNA into rat epidermis *via* local injection, but only a few keratinocytes could express C7 with limited maintenance for about one week⁶³. In another study, the whole 32 kb human COL7A1 was delivered *via* the microinjection of plasmid vectors, and the secretion of procollagen VII was confirmed to be detectable for up to one year⁶⁴. To optimise the plasmid vector for COL7A1 transfection, Ortiz-Urda et al. developed a non-viral vector system based on the Φ C31 bacteriophage integrase system⁶⁵. Primary keratinocytes from patients with RDEB were transfected with Φ C31 integrase-

encoding plasmid containing COL7A1 cDNA sequence. The treated cells displayed the restoration of full-length C7 expression 14 days post transfection. By grafting the COL7A1-transfected cells to immune-deficiency mice, regular level of C7 expression, dermal-epidermal cohesion and AFs regeneration was achieved and maintained for 14 weeks⁶⁵. The non-viral vector presented the promising potential for RDEB treatment, with low biosafety risk, low cytotoxicity and more adaptable to the large gene transfer compared to viral vectors.

1.1.3 Current Ongoing Clinical Trials for EB

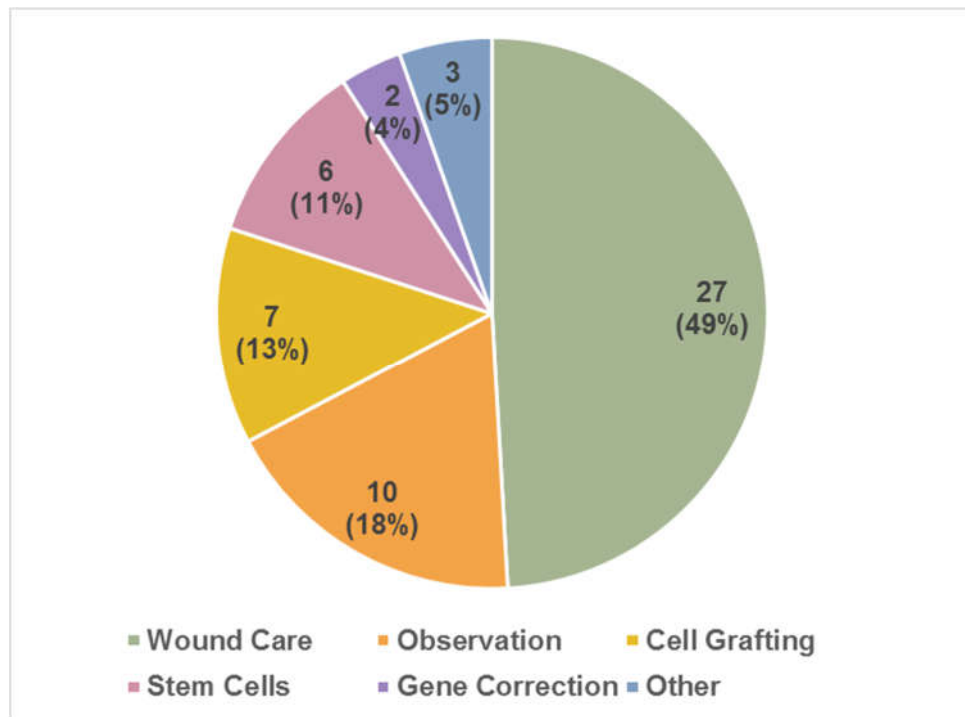


Figure 1. Statistics of different therapies on clinical trials related to EB. Data was collected from <https://www.clinicaltrials.gov> by November 2016.

Currently, over 50 clinical trials related to EB have been studied or on-going (<https://www.clinicaltrials.gov>). Most of them are focused on wound care methods, and some are observational investigations aiming at patients' data collection (**Figure 1**).

Two autologous fibroblasts therapy studies are ongoing, both of which are related to lentiviral vector transduction approaches. Three groups are related to BM-MSK therapy. In Stanford University, a personalised treatment study in Phase I/II combining gene therapy and cell therapy is recruiting participants.

Table 1 provides an update of current ongoing interventional clinical trials specifically for EB treatments, which are all in the status of recruiting participants (<https://www.clinicaltrials.gov>). Aside from topical wound care and symptom alleviation, the clinical studies are focused on allogeneic stem cell transplanting, and gene engineered autologous fibroblasts.

Table 1. Ongoing clinical trials on EB (November 2016, www.clinicaltrials.gov)

Study title	A Phase 1 Clinical Study to Evaluate the Safety of ALLO-ASC-DFU in the Subjects With Dystrophic Epidermolysis Bullosa
Study synopsis	To evaluate ALLO-ASC-DFU, a hydrogel sheet containing allogenic adipose-derived mesenchymal stem cells for dressing DEB wound.
Condition and phase	DEB; Phase 1
Sponsor	Anterogen Co., Ltd.
Study start date	Oct. 2015
Study title	A Phase 1 Study to Evaluate the Safety, Pharmacokinetics and Therapeutic Effect of Topical BPM31510 3.0% Cream in Patients With Epidermolysis Bullosa
Study synopsis	To investigate the effects of a topical cream administered on lesions of EB patients over 12.
Condition and phase	EB; Phase 1
Sponsor	University of Miami
Study start date	Jul. 2016

Study title	Biochemical Correction of Severe Epidermolysis Bullosa by Allogeneic Stem Cell Transplantation
Study synopsis	To estimate the event-free survival rate by 1 year post-transplant with an event defined as a death or failure to have a demonstrable increase in collagen, laminin, integrin, keratin or plakin deposition by 1 year post-transplant or other biochemical, structural or physical measure of improvement.
Condition and phase	EB; Phase 2
Sponsor	Masonic Cancer Center, University of Minnesota
Study start date	Jan. 2010
Study title	A Phase 3, Multi-center, Randomized, Double-Blind, Placebo Controlled Study of the Efficacy and Safety of SD-101 Cream in Patients With Epidermolysis Bullosa
Study synopsis	To assess the efficacy and safety of SD-101-6.0 cream versus SD-101-0.0 (placebo) applied topically in the treatment of patients with EB.
Condition and phase	EB; Phase 3
Sponsor	Scioderm, Inc.
Study start date	Mar. 2015
Study title	A Phase 1/2A Single Center Trial of Gene Transfer for Recessive Dystrophic Epidermolysis Bullosa (RDEB) Using the Drug LZRSE-Col7A1 Engineered Autologous Epidermal Sheets (LEAES)
Study synopsis	To achieve proof-of-concept for a cell-based gene therapy approach in humans with RDEB using patient's genetically engineered cells to graft onto them.
Condition and phase	DEB,EB; Phase 1,2
Sponsor	Stanford University
Study start date	Dec. 2010
Study title	Phase I Study of Lentiviral-mediated COL7A1 Gene-modified Autologous Fibroblasts in Adults With Recessive Dystrophic Epidermolysis Bullosa
Study synopsis	To assess the safety of intradermal injections of gene-modified autologous fibroblasts in 5-10 adults with RDEB.
Condition and phase	RDEB; Phase 1
Sponsor	King's College London
Study start date	Sep. 2015

Study title	A Comparative Study of the Healing of Chronic Skin Ulcers of Recessive Dystrophic Epidermolysis Bullosa : Standard Dressing Versus Amniotic Membrane
Study synopsis	To evaluate the efficacy of the amniotic membrane on the healing of chronic ulcers RDEB on the percentage ulcerated surface re-epithelialized at 12 weeks (M3) from the start of treatment.
Condition and phase	RDEB; Phase 3
Sponsor	Assistance Publique - Hôpitaux de Paris
Study start date	Jan. 2015
Study title	MT 2015-20: Biochemical Correction of Severe Epidermolysis Bullosa by Allogeneic Cell Transplantation and Serial Donor Mesenchymal Cell Infusions
Study synopsis	To determine the event-free survival at 1 year post allogeneic transplant and serial mesenchymal stem cell (MSC) infusions from a related donor (HLA identical, mismatched or haploidentical) or matched unrelated donor for the biochemical correction of severe EB.
Condition and phase	EB; Phase 2
Sponsor	Masonic Cancer Center, University of Minnesota
Study start date	Mar. 2016
Study title	A Phase I/II Study of FCX-007 (Genetically-Modified Autologous Human Dermal Fibroblasts) for Recessive Dystrophic Epidermolysis Bullosa (RDEB)
Study synopsis	To evaluate the safety, influence on C7 expression, presence of anchoring fibrils and wound healing for FCX-007, a genetically modified autologous fibroblasts, administered in subjects with RDEB.
Condition and phase	RDEB; Phase 1,2
Sponsor	Fibrocell Technologies, Inc.
Study start date	Jun. 2016

Study title	A Phase I/II Study Evaluating Allogeneic Mesenchymal Stromal Cells in Adults With Recessive Dystrophic Epidermolysis Bullosa
Study synopsis	To assess whether intravenously administered third-party bone marrow-derived mesenchymal stromal cells (MSCs) are safe and have an impact on disease severity in RDEB.
Condition and phase	RDEB; Phase 1,2
Sponsor	King's College London
Study start date	Jun. 2015
Study title	Study of Epidermal Grafting Using the CelluTome Epidermal Harvesting System for the Treatment of Individual Lesions in Persons With Epidermolysis Bullosa [MT2015-36]
Study synopsis	To investigate the local wound therapy for EB patients using epidermal skin grafting from the same donor that provided the hematopoietic graft, or from the same EB individual with a mosaic (naturally gene corrected) skin, by using a FDA approved vacuum device CelluTome® that enables painless, bloodless and scar-free harvesting of epidermis.
Condition and phase	EB
Sponsor	Masonic Cancer Center, University of Minnesota
Study start date	Aug. 2016
Study title	A Phase 2 Trial of Neurokinin-1 Receptor Antagonist for the Treatment of Itch in Epidermolysis Bullosa Patients
Study synopsis	To determine whether daily oral administration of VPD-737 (5 mg), a drug that has been shown to reduce severe itch on 257 adult patients with chronic pruritus, is effective and safe in adolescents and adults with EB.
Condition and phase	EB; Phase 2
Sponsor	Jean Yuh Tang
Study start date	Jul. 2016

1.1.4 Minicircle Gene Therapy for RDEB

1.1.4.1 Plasmid DNA Vectors

For the purpose of compensating the drawbacks of viral vector on gene therapy, non-viral plasmid vectors have been studied for decades⁶⁶. The plasmid vector is more tolerated to target gene and arises less immune response compared to viral vectors⁶⁷. The plasmid vector is modified to allow protein expression in eukaryotic cells, which eliminates the problem of protein glycosylation in prokaryotic cells⁶⁸. In general non-viral gene therapy procedures, the selected gene of interest is cloned into a plasmid vector backbone, and then the plasmid is transformed into a bacterial host, typically *Escherichia coli* (*E. coli*). The amplification of the plasmid gene can be achieved by culturing the bacterial host. Finally, the host cells are lysed, and the plasmid is purified as biopharmaceutical grade. There are two major functional units in a common plasmid vector: a bacterial backbone and a eukaryotic expression cassette (**Figure 2**).

The bacterial backbone provides the plasmid amplification capability in the bacterial host, which includes the sequence origin of replication and the selection marker. The origin of replication (*ori*) is a sequence for initiating the plasmid replication, which exists both in prokaryotes and eukaryotes. The types of *ori* vary from species. Some *ori* with high copy numbers such as ColE1 and pMB1 are commonly used in the construction of therapeutic plasmid to increase the yield⁶⁹. However, these replication sequences have shown negative effects on the binding of eukaryotic transcription factors⁷⁰ and reduced the expression of targeted gene in eukaryotic cells⁷¹. The selection marker is necessary to purify the targeting plasmid products. Different approaches have been used as selection markers such as antibiotic resistance, auxotrophic complementation⁷², repressor titration^{73,74}, protein based antidote/poison selection schemes⁷⁵ and RNA based selectable markers^{76,77}. The most commonly utilised type is antibiotic resistance markers (ARMs). The addition of specific antibiotic which

matches the resistance on the plasmid pushes the bacteria host to keep the targeting plasmid inside the bacteria so that the targeting plasmid can be amplified accompanied with bacteria replication. However, ARMs may raise negative effects on therapeutic efficiency by triggering high immune response to silence the targeting gene. In addition, the antibiotic resistance gene may be transmitted to the patient's intestinal bacteria with unexpected safety risk^{78,79}.

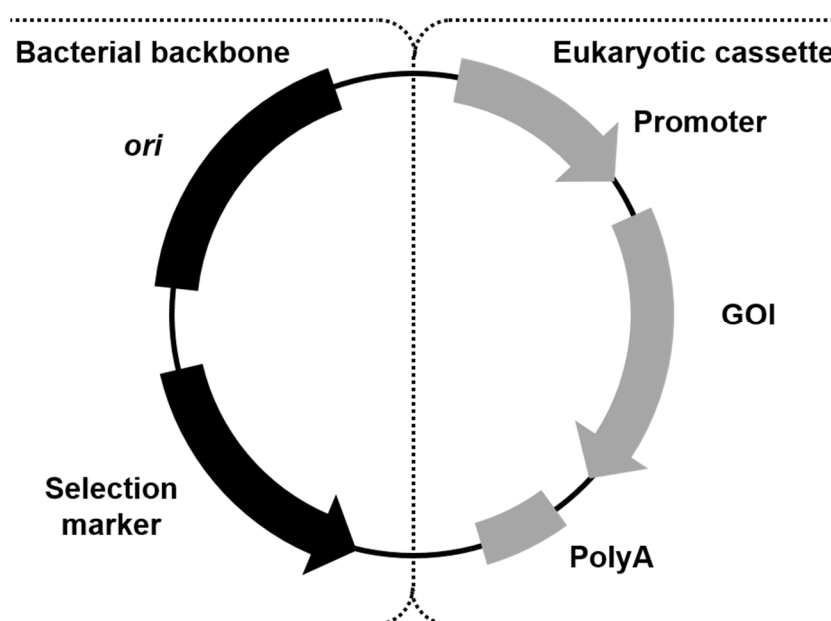


Figure 2. A schematic representation of a generic therapeutic plasmid DNA vector. The bacterial backbone includes the origin of replication (*ori*) and selection marker, which are required for vector amplification in bacterial host. The eukaryotic cassette includes a eukaryotic promoter, the gene of interest (GOI) and a termination polyadenylation signal (polyA), which provide the plasmid desired functionalities.

The eukaryotic expression cassette allows the plasmid expressing the targeted functional gene in eukaryotic cells, which includes a eukaryotic promoter, a polyadenylation terminator and the gene of interest. To elicit RNA transcription of the therapeutic gene in patients, a proper eukaryotic promoter should be located upstream

the gene of interest. Common promoters used in gene therapies include human cytomegalovirus (CMV), simian virus (SV40), human ubiquitin C (UbC), and human elongation factor-1 α (EF-1 α) promoters⁸⁰. The CMV promoter is one of the most studied promoters due to its high-level constitutive expression, non-carcinogenic source and tissue promiscuity⁸¹, but it may enhance antigen expressing in some tissues⁸². The gene of interest (GOI) is the desired DNA sequences for therapeutic targeting gene. In some cases, the gene of interest can be altered with consent codons to achieve a better expression of targeted protein^{83,84}. The polyadenylation (polyA) signal (or named as transcriptional terminator) is usually added to the end of transcription⁸⁵. It is essential for mRNA 3'-end cleavage and polyadenylation in the production process of pre-messenger RNA, for promoting downstream transcriptional termination and for enhancing the stability of mRNA^{86,87}. Bovine growth hormone (BGH), SV40 and human β -globin are commonly used for the gene delivery vectors⁸⁰.

1.1.4.2 Minicircle Vectors

Besides the significant progress achieved on the plasmid vectors for gene therapies, the inevitable drawbacks restrict their applications in RDEB treatments. One of the major issues is that the large size of COL7A1 gene is difficult to fit plasmid vectors. The larger plasmid is easier to be sheared in cells *in vivo* and more difficult to be compressed into cells, which may enhance the nonspecific DNA toxicity and reduce the efficiency of gene transfection and expression⁸⁸. On the other hand, the bacterial backbone occupies about half size of the whole plasmid, which only helps on the plasmid amplification but does not contribute to its therapeutic functionalities. It may rise unnecessary immunogenicity and eukaryotic transcriptional silencing, which is detrimental to the therapeutic gene expression⁸⁹. Therefore, efforts have been devoted to removing the bacterial backbone and reduce the size of the plasmid to improve the gene transfection and targeted protein expression.

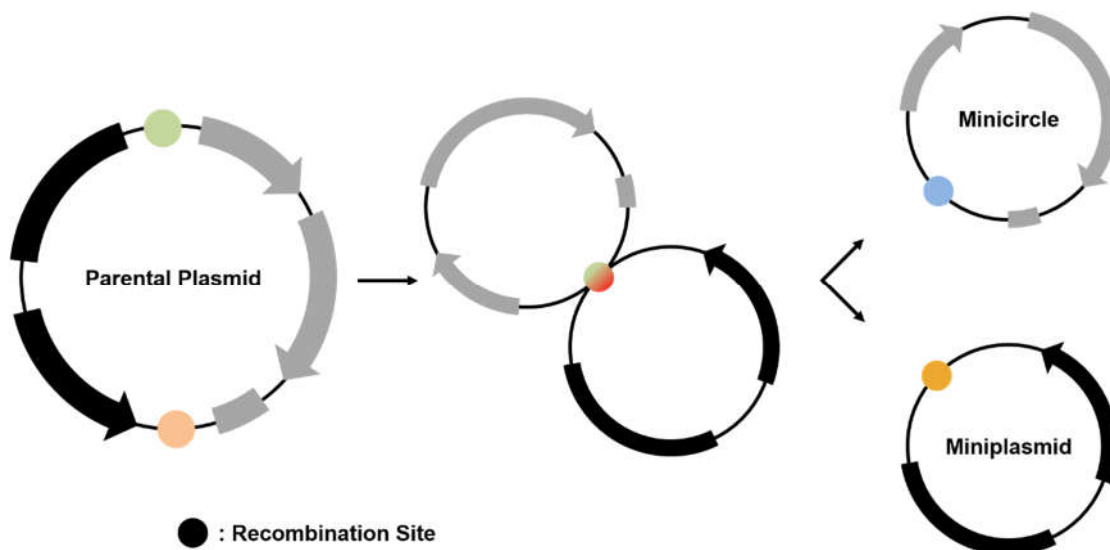


Figure 3. Schematic representation of minicircle vectors. The minicircle vectors are modified from plasmid vectors, with the eliminating of bacterial backbones through the recombination of two specific sites flanked by eukaryotic expression cassette.

Minicircles are a type of non-viral gene delivery vectors modified from plasmid vectors, in which lacking origin of replication and selection marker from the original bacterial backbone (**Figure 3**). In 1997, Darquet et al. did the pioneering work on the design and production of minicircle DNA vectors⁹⁰. These minicircles were produced from constructed plasmid pXL2650, consisting of a phage λ integrase, ColE1 origin of replication, ampicillin resistance gene *galK* and a luciferase gene expression cassette (*luc*). The bacterial regions of ColE1 and *galK* were excised by site-specific recombination *via* the phage λ integrase between *attB* and *attP* sites, resulting in the separation of the plasmid to minicircle and miniplasmid (bacteria backbone). The *attB* and *attP* sites are two short sequences from the phage λ genome and the *E. coli* chromosome respectively, which were used to integrate the circular phage genome into the *E. coli* chromosome⁹¹. The minicircle DNA showed higher transgene expression efficiency than the parental plasmid. However, in this preliminary study, there were about 40% of plasmids failed to be recombined and approximate 30% dimers

formation⁹⁰.

To improve this system, Kreiss et al. introduced the *par* genes that belong to an efficient partitioning system to resolve multimeric forms of minicircle⁹². It was demonstrated up to 38% increased production of minicircle monomers. With the aim to increase the rate of monomeric minicircle products, Bigger et al. reported a *cre/loxP* system in 2001⁹³. The *Cre* recombinase is a bacteriophage P1-derived tyrosine integrase that could catalyse the bi-directional, site-specific recombination between two 34-base-pair *loxP* sites. After recombination, the plasmid was separated into two DNA molecules, and each molecule contains a single *loxP* site. To prevent the reversion, one *loxP* half-site was reconstructed to lose its activity after recombining with a corresponding wild-type *loxP*. In this study, the *loxP* sites, the *Cre* recombinase gene sequence and the bacterial strains were modified to increase the yield of targeted proteins. However, many concatemers were formed accompanied by the minicircle production, and contamination of parental plasmid and miniplasmid residues are difficult to be removed from the system that may elicit a higher immune response in the clinical application⁹³. Further, Chen et al. introduced a Φ C31 integrase-mediated system, showing more efficient yield compared to previous *Cre* recombinase⁹⁴. The minicircle was constructed by recombination between *attB* and *attP* sites in this study. The expression level of targeted protein was over 10-fold higher by the minicircle DNA versus linear expression cassette. The minicircle vector has also prevented the transcriptional silencing effect⁹⁴. Another widely studied approach is based on a serine recombinase of ParA resolvase with two identical hybrid resolution sites which can be broadly applied in both prokaryotic and eukaryotic hosts⁹⁵. ParA resolvase is more efficient under the control of pBAD/AraC L-arabinose inducible system. With the absence of L-arabinose in the bacteria growing culture, the transcription of ParA gene is repressed by AraC to slow down the synthesis and functioning of ParA resolvase. After sufficient time for the amplification of bacterial host and parental vectors, with the addition of L-arabinose, the expression of ParA resolvase is stimulated by the araBAD operon.

Mayrhofer et al. first used this system in *E. coli* K12 strain for minicircle production, following affinity chromatography purification realised by the bio-recognition between Lac I in the column and lactose operator sites (LacOs) in the minicircle vectors. With the optimisation of minicircle production and purification, it was more suitable for minicircle scale-up manufacture⁹⁵.

In above studies, the minicircles were purified from the plasmid backbone through the restriction enzyme digestion and caesium chloride (CsCl) density-gradient ultracentrifugation, which need multiple steps with time- and labour-consuming. For the first time, Kay's group introduced an endonuclease I-Sce I gene into the minicircle producing plasmid based on Φ C31 integrase system to degrade the bacterial backbone, which remarkably increased the yield of minicircle products⁹⁶. Further improvement was applied by specific genetic modification of *Escherichia coli* and inserting ten copies of Φ C31 integrase and six copies of I-Sce I endonuclease sites⁹⁷. By reducing the temperature when cultivating enough time after L-arabinose induction, the activity of I-Sce I endonuclease was relatively enhanced compared with Φ C31 integrase activity so that remaining parental plasmid and miniplasmid could be eliminated by the end of the amplification process. By using this system, the yield of minicircle production was increased 3-5 times, and the contamination rate of plasmid DNA was decreased ten times compared to previous strategies. Additionally, the cost of minicircle production by this method is as low as traditional plasmid production process.

1.2 Hypotheses and Objectives

The goal of this thesis is to develop an efficient non-viral minicircle DNA vector for COL7A1 delivery and achieve the long-term secretion of functional type VII collagen in RDEB cutaneous cells. It was hypothesised that minicircle vector, without prokaryote origin of replication and antibiotic resistance gene, can significantly reduce the size of

transplanted gene, increase the transfection efficacy and prolong the type VII collagen expression *in vitro*.

The whole project was divided into two phases with specific objectives and hypotheses.

Objective One:

To evaluate and optimise the transfection methodology of a commercially available minicircle vector with a reporter gene in different cell types.

Hypotheses: Minicircle vectors produced by Φ C31 integrase system can be efficiently transfected into different types of cells and present long-term expression *in vitro*. Optimised methodology can be achieved by choosing proper transfect reagents and varying the DNA/reagent ratio for different cells.

Objective Two:

To construct a minicircle system with COL7A1 gene, and evaluate its transfection efficiency and the long-term expression of C7 in RDEB cells.

Hypotheses: Full-length COL7A1 gene can be introduced into a minicircle vector. Reduced gene size and lack of prokaryote origin can significantly increase the transfection efficiency and prolong the expression of type VII collagen in human RDEB keratinocytes.

Chapter Two

Materials and Methods

2.1 Materials

Normal human keratinocyte (NHK) and immortalised RDEB keratinocyte (RDEBK) cell lines were kindly provided by Dr Larcher F. (Epithelial Biomedicine Division, Cutaneous Disease Modelling Unit, CIEMAT, Madrid, Spain). pcDNA3.1/COL7A1 plasmid DNA was kindly provided by Dr South A. (Medical Research Institute, College of Medicine, Dentistry, and Nursing, University of Dundee, Dundee, UK). Minicircle construction system was purchased from System Biosciences (Mountain View, CA, USA). A comprehensive list of materials has been supplied in Appendix II-A.

2.2 Methods

2.2.1 Minicircle Amplification and Purification

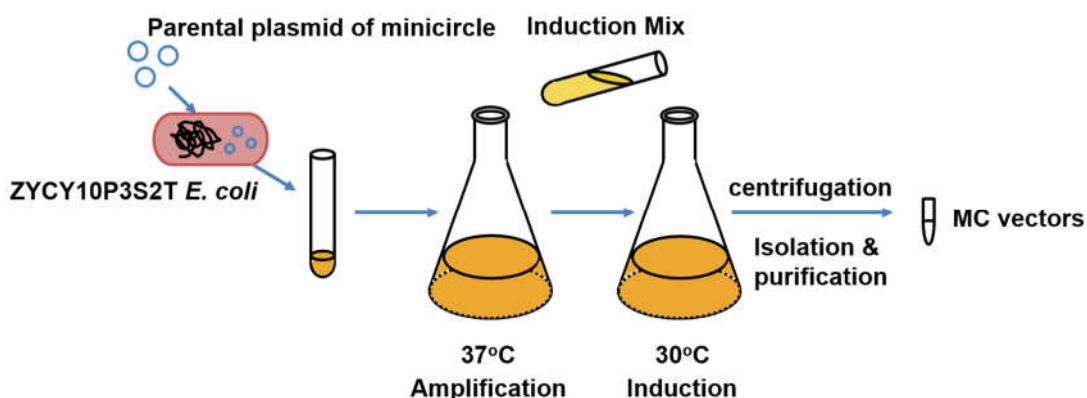


Figure 4. Minicircle production procedures.

Constructed minicircle DNA was produced according to the recommended protocol. Briefly, ZYCY10P3S2T *E. coli* was firstly transformed with constructed parental

plasmid and grown in 5 mL lysogeny broth (LB) with Kanamycin (50 µg/mL), followed by re-inoculation to 400 mL terrific broth (TB) (Kanamycin) to culture overnight at 37 °C. The culture was then mixed with 400 mL LB, 16 mL 1N sodium hydroxide and 400 µL 20% L-arabinose, and inducted at 30 °C for 8 hours followed by standard centrifugation. The pellets were harvested and the minicircle product was purified using the QIAGEN® Plasmid Mega Kit. Schematic diagram of the procedures is as **Figure 4** shown.

2.2.2 Construction of Minicircle Vector with COL7A1 Expression Gene

Full-length cDNA of human COL7A1 was digested by *EcoR* I from pcDNA3.1/COL7A1 and inserted into MN512 (with red fluorescence protein expression gene, RFP) parental plasmid (PP) as PP-COL7A1 vector.

2.2.3 Cell Cultures

Hela cells were cultured in Dulbecco's Modified Eagle Medium (DMEM) with 10% fetal bovine serum (FBS) and 1% Penicillin-Streptomycin (P/S). NHK and RDEBK were cultured in Keratinocyte Basal Medium (KBM) with PromoCell kits and 1% P/S. Cells were incubated at 37 °C in a humidified atmosphere with 5% carbon dioxide.

2.2.4 Cell Transfection

In minicircle transfection efficiency observation, 8,000 cells/well were seeded in 96-well plates. In flow cytometry experiments, cells were seeded in 6-well plates at a density of 200,000 cells/well. In type VII collagen expression experiments, cells were seeded in 15 cm dishes with 1.5 million cells per dish. All transfections were operated with Xfect™ and Lipofectamine® 2000 commercial transfection reagent.

2.2.5 Fluorescence Detection and Flow Cytometry

GFP and RFP fluorescence was detected using an OLYMPUS-X41 microscope. At

specific time points post transfection, transfected cells were visualised directly under the microscope *via* blue or green spectral filter.

For flow cytometry analysis, cells were firstly trypsinized once getting confluent. Then 1/10 of cells were centrifuged and re-suspended in fresh medium. Propidium iodide was added to cell samples for the staining of dead cells. GFP fluorescence was excited by 488 nm laser and detected at 565-605 nm. 8,000 cells were detected for each sample. Finally, 200,000 cells were seeded back to a fresh culture plate.

2.2.6 Western Blotting

Cell supernatants were harvested every three days and concentrated to ~300 μ L by Amicon Ultra-15 Centrifugal Filter Units. Concentrated samples were denatured with 5x sample buffer at 98 °C, and run on a polyacrylamide gel (6% running gel, 3% stacking gel) with equal amounts of total protein. The primary antibody (rabbit anti-human type VII collagen poly-antibody) worked on 1:4000 dilution. The secondary antibody (anti-rabbit IgG with HRP-linked) was detected through Pierce ECL Plus Western Blotting Substrate and with exposure.

Detailed protocols for all the experiments have shown in Appendix II.

Chapter Three

Results and Discussion

In this study, we conjugated COL7A1 gene with a commercially available Φ C31 minicircle system. Several types of cells were transfected with the minicircle (MC) vector loaded with GFP or RFP reporter gene and COL7A1 gene. With optimised transfection methodology, we have demonstrated an improved transfection efficiency and long-term expression of the MC vectors compared to the parental plasmid (PP). The type VII collagen (C7) expression in human RDEB mutated keratinocytes was significantly promoted by the MC vectors, which showed promising potential for RDEB treatments.

3.1 Minicircle DNA Production and Characterisation

3.1.1 Production of Minicircle Vector with Reporter Gene

The PP vector is a circular double-stranded DNA plasmid with the size around 7 kb (**Figure 5**). The bacterial backbone includes a pUC origin of replication and a Kanamycin resistance marker gene. 32 x *Sce*-I sites are located next to the origin of replication for the degradation of the bacterial backbone. The hybrid sites of *attP* and *attB* flank the bacterial backbone. In the expression cassette, gene of interest can be inserted downstream a high-level continuous expressing CMV promoter. Next to the gene of interest, there is a green or red fluorescence protein gene (GFP/RFP) guided by EF1 α promoter as a reporter of expression. At the end of the expression cassette, a polyadenylation signal SV40 is placed for the production of mature mRNA in eukaryotic cells. The bacteria backbone (~4 kb) occupies more than half of the whole PP. During the inducing process of MC production, site *attP* and *attB* are recombined to form new sites of *attR* and *attL*, resulting in the separation of bacterial backbone and

expression cassette, forming two circles of miniplasmid (MP) and MC. The size of the MC vector is shrunk to about 3 kb. As **Figure 6** shown, the size of the PP and MC DNA were indicated by electrophoresis analysis on 0.8% agarose gels. Lane 1 presents the size of original PP and Lane 2 presents the MC, which indicates the MC vector is about 4 kb smaller than the PP.

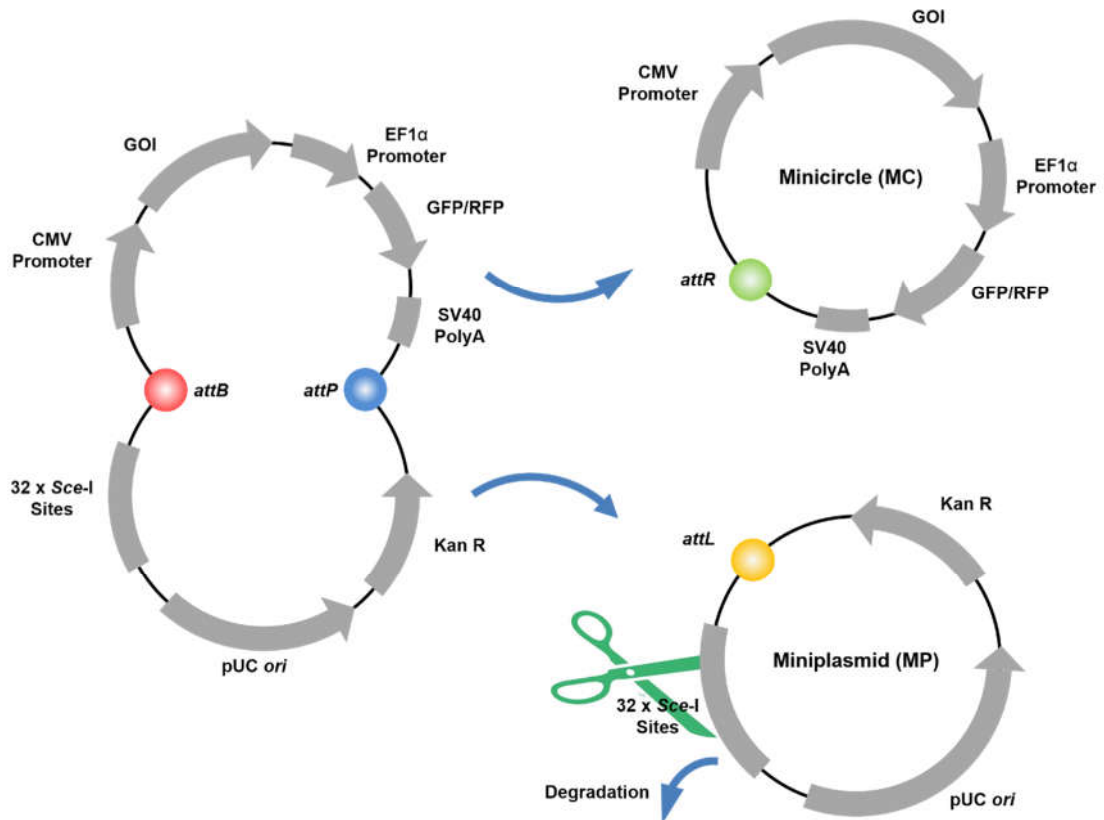


Figure 5. Schematic representation of Φ C31 recombinase/I-Sce I endonuclease minicircle system vector. The hybridization of recombinase binding sites of *attP* and *attB* forms one minicircle (MC) molecule, and a miniplasmid (MP) molecule that can be degraded by the activation of I-Sce I endonuclease.

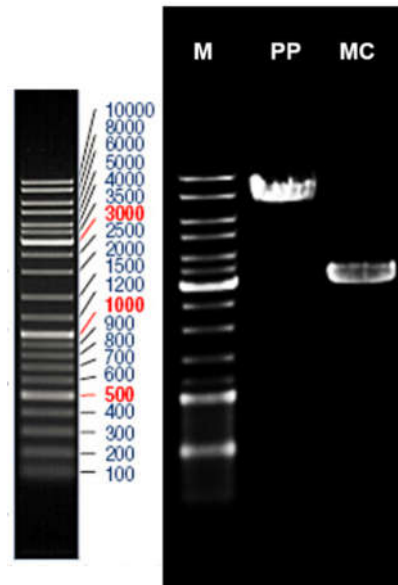


Figure 6. DNA electrophoresis of the PP and MC vector. Lane 1: parental plasmid (PP) (~7 kb); Lane 2: minicircle (MC) (~3 kb); M: standard DNA ladder.

3.1.2 Optimisation of Minicircle Delivery Methodology

A number of gene delivery methodologies have been developed to assist non-viral DNA vector transfection. For example, physical approaches can be used to help naked DNA transfer into cells, such as electroporation^{98,99}, ultrasound^{100,101}, hydrodynamic pressure^{102,103}, and gene gun^{104,105}. However, most physical approaches are difficult to be applied to humans and for systemic gene delivery applications¹⁰⁶. In contrast, chemical transfection reagents have been widely studied such as cationic lipids¹⁰⁷, cationic polymers¹⁰⁸, polymersomes¹⁰⁹, cell-penetrating peptides¹¹⁰ and inorganic nanoparticles¹¹¹. These reagents can condense negative-charged DNA into small particles on quasi-steady state, get into cells *via* endocytosis, help DNA to prevent destruction by lysosome and release DNA in time¹¹². In this study, we chose two different commonly used commercially available transfection reagents of Lipofectamine® (cationic lipids based) and Xfect™ (cationic polymer based) to compare the transfection efficiency of the PP and MC vectors. Vectors with GFP

reporter gene (MN511, System Biosciences, CA, USA) were utilised in this section instead of RFP due to its quicker expression response.

Transfection via Lipofectamine® 2000 Reagent

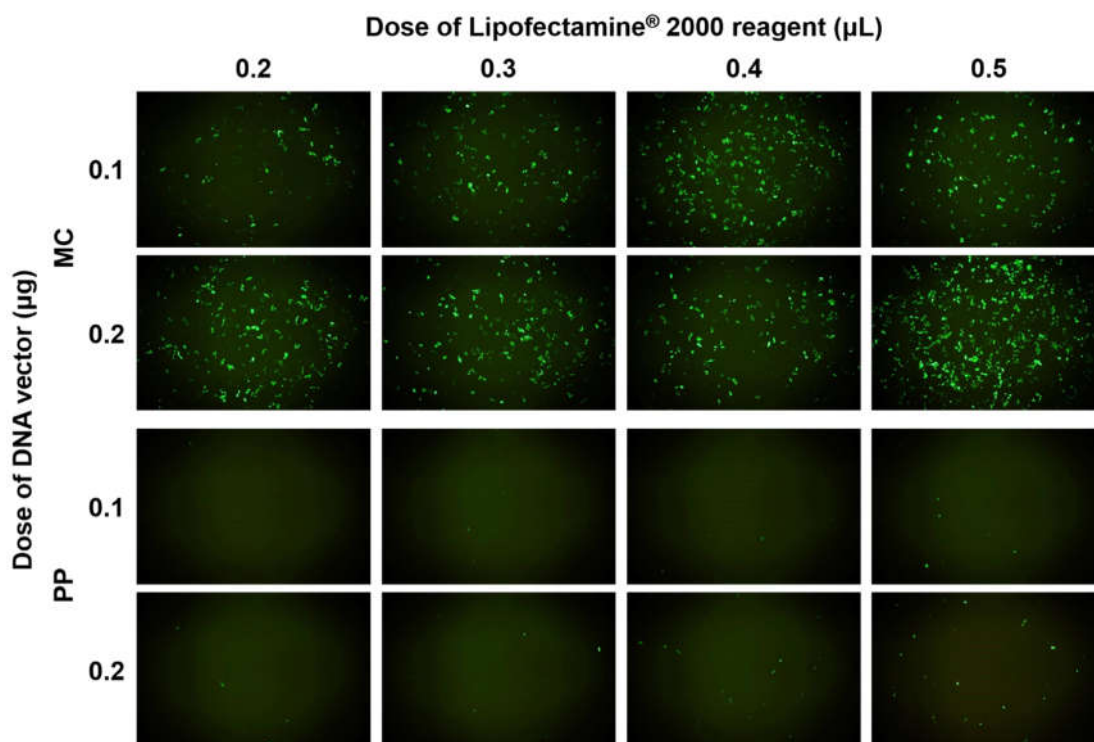


Figure 7. Evaluation of the transfection efficiency of the MC and PP vectors with GFP reporter in HeLa cells *via* Lipofectamine® 2000 reagent. Different doses of Lipofectamine® 2000 reagent (0.2 to 0.5 μL) and loading DNA amount were used to optimise the transfection recipe. The photos were taken under 4x objective.

The MC and PP vectors were produced following the procedure as **Figure 4** shown. Two commonly used cell lines, HeLa cells and 3T3 mouse fibroblasts, were utilised to evaluate the vectors' transfection efficiency and long-term expression. Cells were plated in 96-well plates. DNA-lipid complexes were prepared as recommended. Different DNA/Lipofectamine® 2000 Reagent ratios and loading DNA amounts (0.1 and 0.2 μg) were tested to optimise the transfection of the MC and PP in targeting cells.

After two days incubation, green fluorescence signal of the transfected cells were determined under fluorescence microscope, which represented the success of transfection into cells. **Figure 7** and **Figure 8** displays the transfection efficiency by the MC and PP in Hela cells and 3T3 cells respectively. It is shown that the higher DNA loading dose (0.2 μg) increases the transfected cell number in both MC and PP treatment groups. The MC shows obvious higher transfection efficiency than the PP vector at all DNA/reagent ratios for both cell types. However, increased number of dead cells were observed when higher DNA and reagent concentrations were used (data not shown), which indicated the Lipofectamine[®] 2000 Reagent was too toxic to these cells. The high cytotoxicity and low DNA usage dose will significantly limit its future application on RDEB treatments.

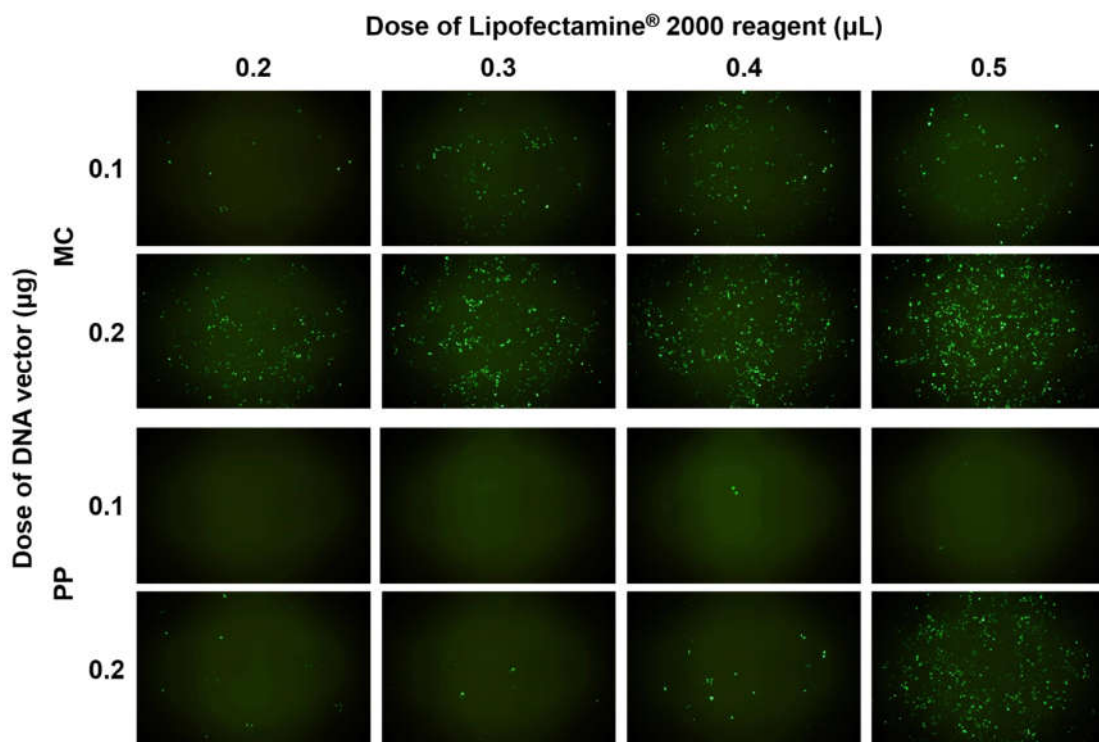


Figure 8. Evaluation of the transfection efficiency of the MC and PP vectors with GFP reporter in 3T3 cells via Lipofectamine[®] 2000 reagent. Different doses of Lipofectamine[®] 2000 reagent (0.2 to 0.5 μL) and loading DNA amount were used to optimise the transfection recipe. The photos were taken under 4x objective.

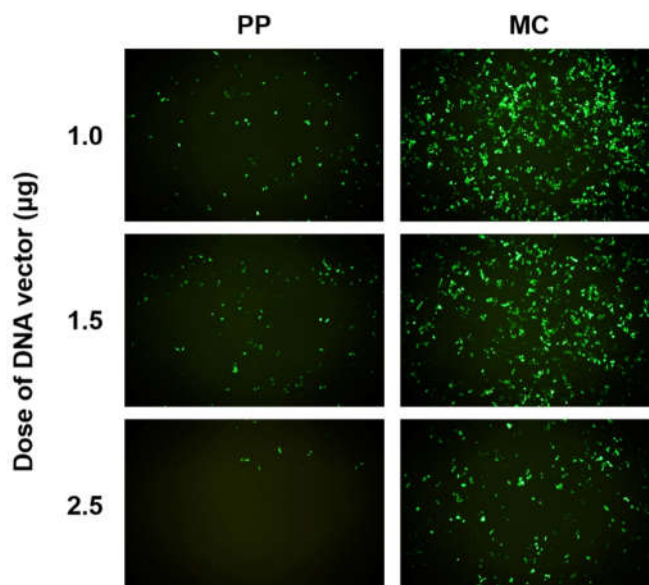
Transfection via Xfect™ Reagent

Figure 9. Evaluation of the transfection efficiency of the MC and PP vectors with GFP reporter in HeLa cells via Xfect™ reagent. Different doses of loading DNA amount (1.0 to 2.5 µg) were used to optimise the transfection recipe. The photos were taken under 4x objective.

The MC and PP vectors were transfected into HeLa and 3T3 cells using a polymer-based transfection reagent of Xfect™. The DNA/polymer ratio was used as recommended. Considering the lower toxicity of the compound, 10-time higher dose of DNA (1.0 µg to 2.5 µg) can be applied on cells compared to Lipofectamine® 2000. The transfected cells were observed under the microscope two days post transfection. Similar trends are exhibited that the MC vectors represent more transfected cells than the PP vectors with the same DNA amount in both HeLa (**Figure 9**) and 3T3 (**Figure 10**) cells. It was found that the transfection efficiency was decreased with increased DNA dose. Meantime, we observed more cells detaching from the bottom in the higher dose (2.5 µg) treatment wells, which showed the toxicity of high concentration Xfect™. Whereas, in the lower dose (1.0 µg) treatment wells, there was no significant difference

of cell death compared with non-transfected control. By comparing the cytotoxicity and transfection efficiency of Lipofectamine® 2000 and Xfect™, we chose Xfect™ for the COL7A1 gene delivery in the following studies.

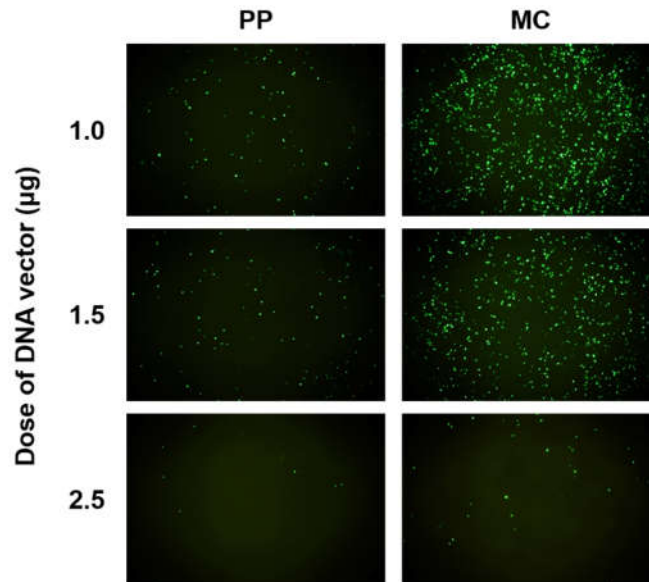


Figure 10. Evaluation of the transfection efficiency of the MC and PP vectors with GFP reporter in 3T3 cells via Xfect™ reagent. Different doses of loading DNA amount (1.0 to 2.5 µg) were used to optimise the transfection recipe. The photos were taken under 4x objective.

3.1.3 Evaluation of Long-Term Gene Expression on MC and PP Vectors

In this section, three types of related cells were used to investigate the long-term gene expression *via* the MC and PP vectors. In normal human skin, type VII collagen is synthesised by keratinocytes and fibroblasts, while keratinocytes produce more than 90% of type VII collagen and form anchoring fibrils (AFs) in the dermal-epidermal junction (DEJ)¹¹³. Over 300 pathogenic mutations have been reported within COL7A1 gene, leading to dominant and recessive DEB¹². One of the most severe subtypes of RDEB mutations (c.6527insC) is caused by the insertion of a cytosine in exon 80 and

form a TAA stop codon in the middle of the COL7A1 gene (337 bp downstream of codon 2176), which results in very few type VII collagen monomers expression¹¹⁴. In this study, we used an immortalised keratinocyte cell lines with the c.6527insC mutation on COL7A1 gene, which was firstly developed from RDEB patients by Chamorro and colleagues¹¹⁵. These immortalised cells were capable of reproducing RDEB phenotypes such as the lack of type VII collagen expression and blister forming between dermis and epidermis region. In addition, the Hela cell line (a commonly used cell line for gene transfection studies) and NHK (normal human keratinocyte cell line) were used as controls.

To compare transfection efficiencies of the PP and MC vectors, an equal mole of the PP and MC DNA were transfected into different cell lines using Xfect™ reagent with optimised procedure as discussed above. Two days post transfection, peak GFP expression was reached across all cell lines with both vectors. Almost all of the Hela cells showed GFP expression (**Figure 11A**); NHK cells were more difficult to transfect (**Figure 12A**); and RDEBK cells showed the lowest transfection efficiency (**Figure 13A**). Across all cell types, it was suggested that more cells were transfected with the MC rather than the PP vector, demonstrating that the use of the MC vector increased transfection efficiency in a variety of cell types. Furthermore, the quantitative results of GFP transfection ratio and expression level were analysed by flow cytometry. Due to the high level of sensitivity of the flow cytometer, it was shown that the number of GFP positive living cells in the MC group was only slightly higher than the PP group. For example, 85.2% of MC transfected Hela cells were GFP-positive versus 80.2% in PP transfected group (n=3) (**Figure 11B**). Nonetheless, the intensity results demonstrated GFP expression level of MC transfected cells were higher compared to the PP group (**Figure 11C**). For Hela cells, the most cells in the MC treated group (red curve) showed an emission intensity higher than 10^5 , and the emission intensity of the most cells in the PP treated group were lower than 10^5 (blue curve). Similar results were seen for NHK (**Figure 12B-C**) and RDEBK (**Figure 13B-C**) cells, indicating that the MC vector

enhanced GFP expression compared to the PP vector. These results suggested the MC vector promoting the gene transfection and expression compared to the PP vectors in tested cells.

Long-term GFP expression by both MC and PP vectors was compared using above cell types by flow cytometry (**Figure 14**). To maintain a normal rate of cell proliferation, cells were trypsinized once getting confluent and re-seeded on fresh culture dishes with diluted cell numbers after flow cytometry measurements. The trypsinization and reseeded of cells significantly reduced the transfected cells and caused a remarkable drop in fluorescence intensity. Even so, roughly 20% of GFP positive Hela cells could be detected in the MC groups after two weeks, while less than 10% was seen in the PP groups. In RDEBK cells, the initial transfection efficiency rate was only roughly 20% for both vectors due to the sensitivity of this diseased cell type. Over half of the GFP-positive cells still maintained after 14 days in the MC group compared to less than 25% in the PP group, demonstrating that the MC vector significantly prolonged the protein expression of the reporter transgene in transfected cells.

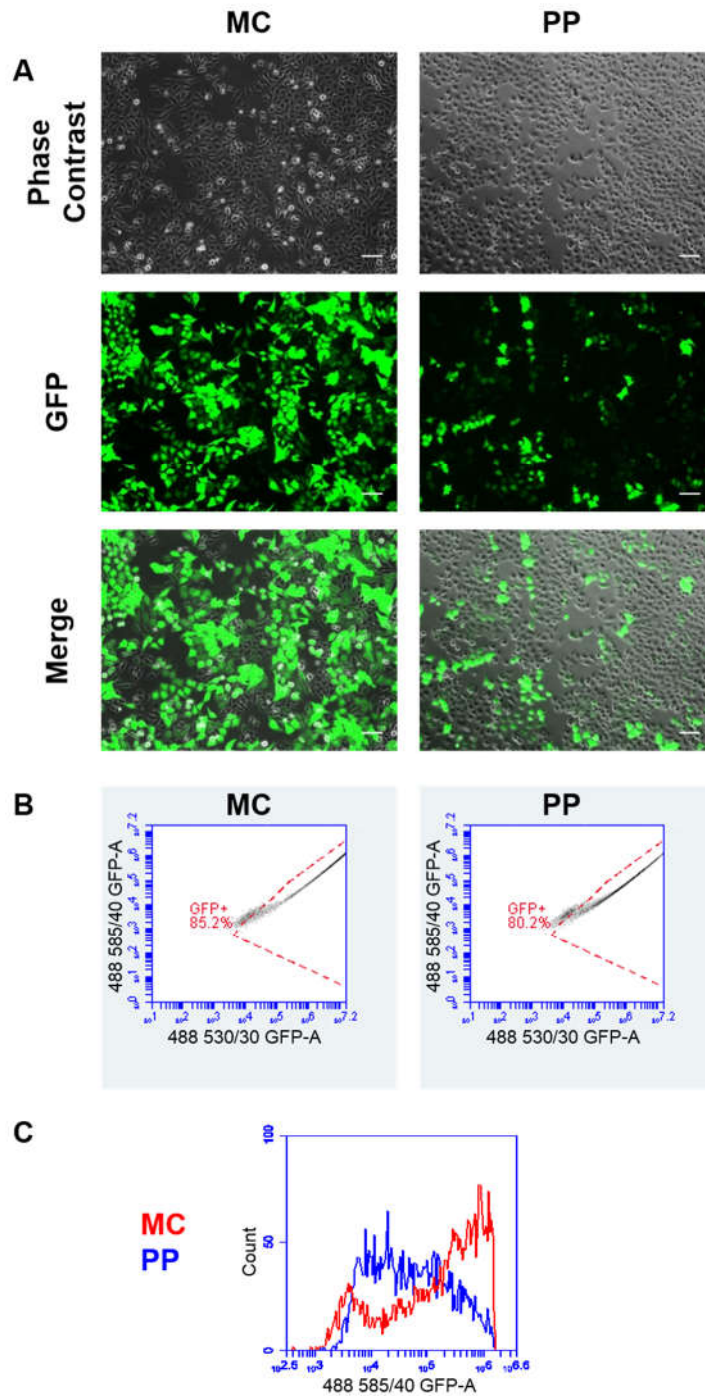


Figure 11. Transfection assessment of the MC and PP vectors in HeLa cells two days post transfection. (A) Fluorescent microscopy images of GFP fluorescence expression. (Scale bars in all cases represent 100 μm); (B) Flow cytometry analysis of GFP-positive cells; (C) GFP intensities by flow cytometry analysis. The red curve represents the MC vector, and the blue curve represents the PP vector.

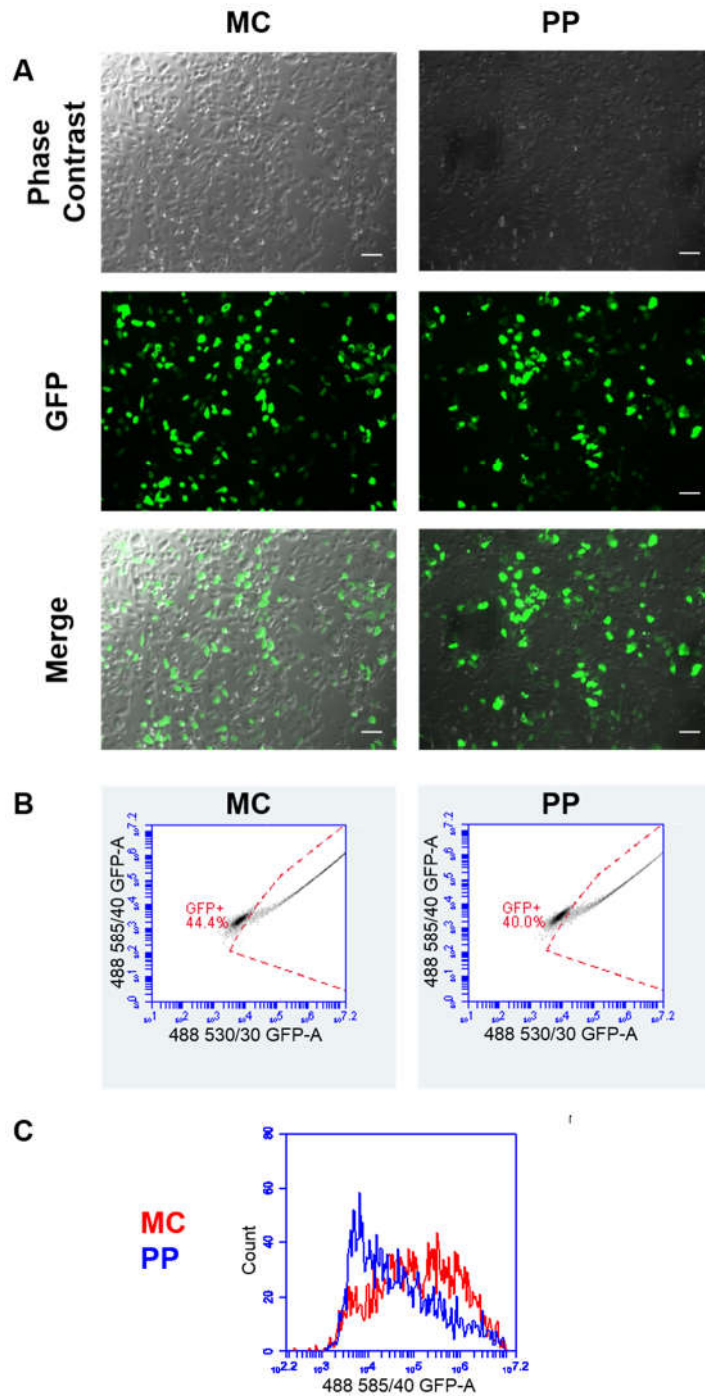


Figure 12. Transfection assessment of the MC and PP vectors in NHK cells two days post transfection. (A) Fluorescent microscopy images of GFP fluorescence expression. (Scale bars in all cases represent 100 μ m); (B) Flow cytometry analysis of GFP-positive cells; (C) GFP intensities by flow cytometry analysis. The red curve represents the MC vector, and the blue curve represents the PP vector.

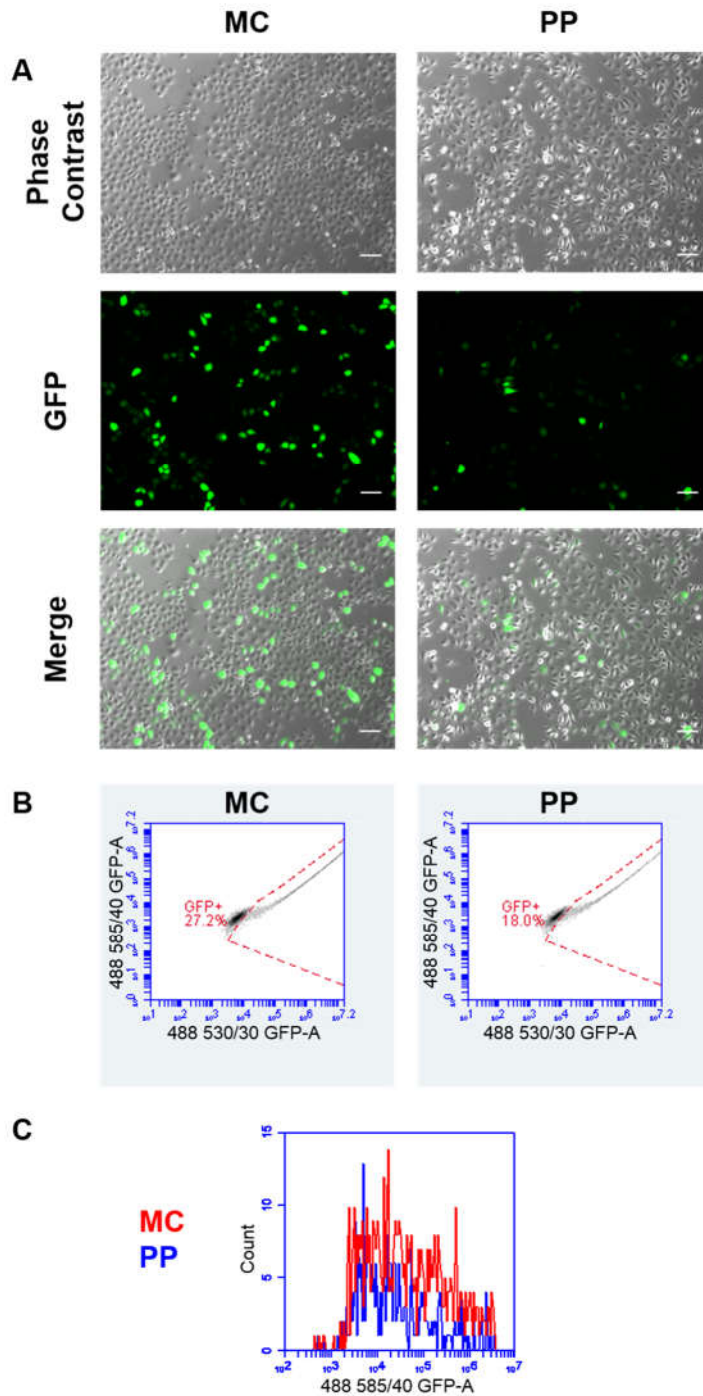


Figure 13. Transfection assessment of the MC and PP vectors in RDEBK cells two days post transfection. (A) Fluorescent microscopy images of GFP fluorescence expression. (Scale bars in all cases represent 100 μ m); (B) Flow cytometry analysis of GFP-positive cells; (C) GFP intensities by flow cytometry analysis. The red curve represents the MC vector, and the blue curve represents the PP vector.

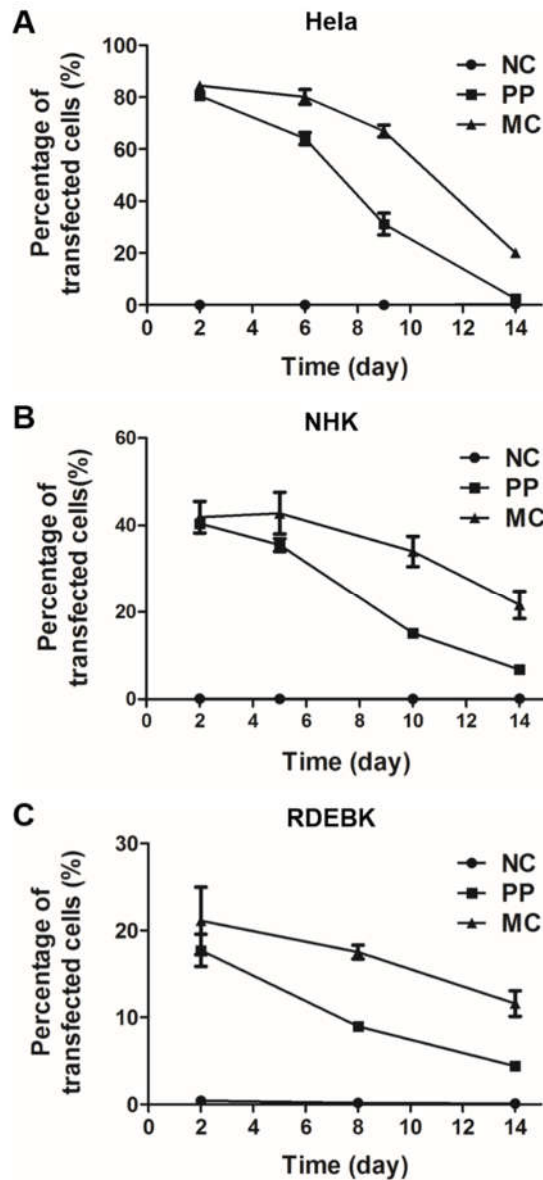


Figure 14. Flow cytometry analysis of transfected GFP positive cells by the PP and MC vectors up to two weeks. Percentage of transfected cells by the PP and MC in (A) HeLa, (B) NHK and (C) RDEBK. NC: negative control of non-transfected cells. (mean \pm SD, n = 3)

3.2 Restoration of Type VII Collagen *In Vitro*

To prevent the blistering between dermis and epidermis that tortures RDEB patients, it is necessary to accomplish the restoration of type VII collagen in cutaneous cells. Type

VII collagen is a very large protein. The human COL7A1 gene expressing type VII collagen includes 32 kb of genomic DNA and consists of 118 exons, resulting in an 8.9-kb mRNA to express procollagen VII containing 2944 amino acids and then forming type VII collagen with the molecular weight of ~293 kDa. We introduced a sequence of double-stranded complementary DNA (8.9 kb) from COL7A1 mRNA into the MC system. Traditional viral or plasmid vectors struggle to accommodate such large genes while maintaining high levels of transfection efficiency with minimal cytotoxicity. The MC system effectively reduces the size of the vector containing COL7A1 transgene by removing the bacterial backbone, which could also aid in reducing its transcriptional silencing, thereby offering an ideal platform for RDEB gene therapy. In this section, the PP and MC vectors with COL7A1 and RFP reporter gene (PP-COL7A1 and MC-COL7A1) were constructed and used to determine the long-term expression of type VII collagen.

3.2.1 Construction of Minicircle-COL7A1 and Parental Plasmid-COL7A1

In this study, we introduced a full-length cDNA of COL7A1 gene downstream the CMV promoter in the MC vector at an *EcoR* I restriction endonuclease digestion site (**Figure 15**). Firstly, the COL7A1 gene was extracted from a pcDNA3.1/COL7A1 plasmid by *EcoR* I digestion (on both ends of COL7A1 gene). Then, the MN512 parental plasmid was also digested with *EcoR* I restriction enzyme, followed by dephosphorylation to prevent self-ligation. The digested products of linear pcDNA3.1 backbone, linear COL7A1 gene and linear MN512 vector, were all mixed and ligated with T4 DNA ligase. The ligation mixture was transformed into ZYCY10P3S2T *E. coli*, and the bacterial host was cultured on agar plates with Kanamycin antibiotic at 37 °C. Then twenty colonies were picked up from the plates and inoculated into 5 mL LB medium with Kanamycin to propagate the positive plasmids. The correctly constructed plasmid (MN512-COL7A1) was identified by DNA electrophoresis after *EcoR* I digestion. As discussed above, the size of COL7A1 gene is as large as 8.9 kb which is difficult to be constructed

into other vectors. Traditional fragment extraction method from agarose gel lead to high risk of large DNA fracture and very low recycle efficiency. In our study, we avoided the gel extraction process by using the different antibiotic resistance properties in MN512 and pcDNA3.1 plasmid, that the pcDNA3.1 plasmid possesses both Ampicillin- and Neomycin-resistance marker, distinct from the Kanamycin marker in MN512 vector. After plasmid digestion, pcDNA3.1 backbones and COL7A1 fragments were all put in the ligation mix, together with MN512 linear backbone. When culturing on Kanamycin agar plates, those plasmids without MN512 backbone segments were screened out, such as pcDNA3.1 self-ligation circle, COL7A1 self-ligation circle, pcDNA3.1-COL7A1, pcDNA3.1-pcDNA3.1 and COL7A1-COL7A1. Besides, the dephosphorylation of linear MN512 avoided the self-ligation. Thus the probability of achieving MN512-COL7A1 products was greatly enhanced among the positive colonies.

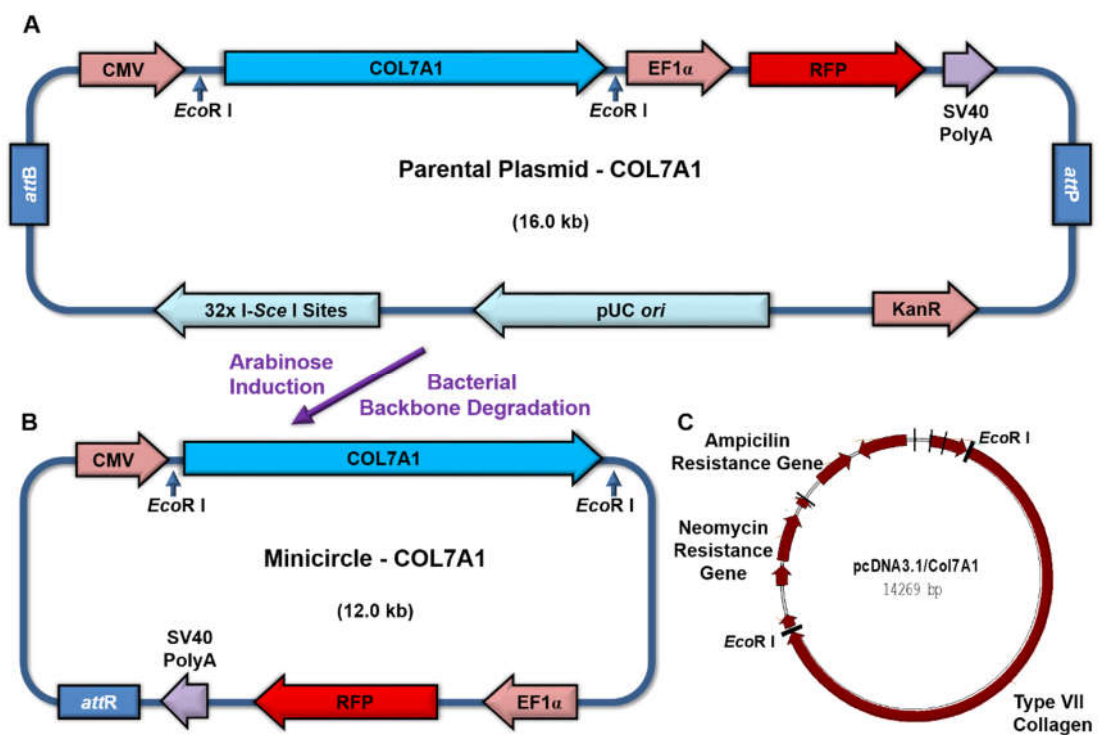


Figure 15. Schematic diagram of (A) parental plasmid-COL7A1 (PP-COL7A1), (B) minicircle-COL7A1 (MC-COL7A1) and (C) pcDNA3.1/COL7A1 vector.

As **Figure 16** shown, PP-COL7A1 and MC-COL7A1 have been successfully constructed. Undigested PP and MC vectors with COL7A1 gene (PP-COL7A1, MC-COL7A1) are shown as Lane 1 and Lane 3, which are seen to be slightly smaller than the real size due to the supercoiled structure of a circle plasmid. After digestion by *EcoR* I, both PP-COL7A1 and MC-COL7A1 were cut into two bands (**Figure 16**, Lane 2 and 4). The upper bands represent the transgene of COL7A1 (~8.9 kb), and the lower bands are the backbones. The COL7A1 gene occupies about 3/4 of the entire MC-COL7A1 vector as expected.

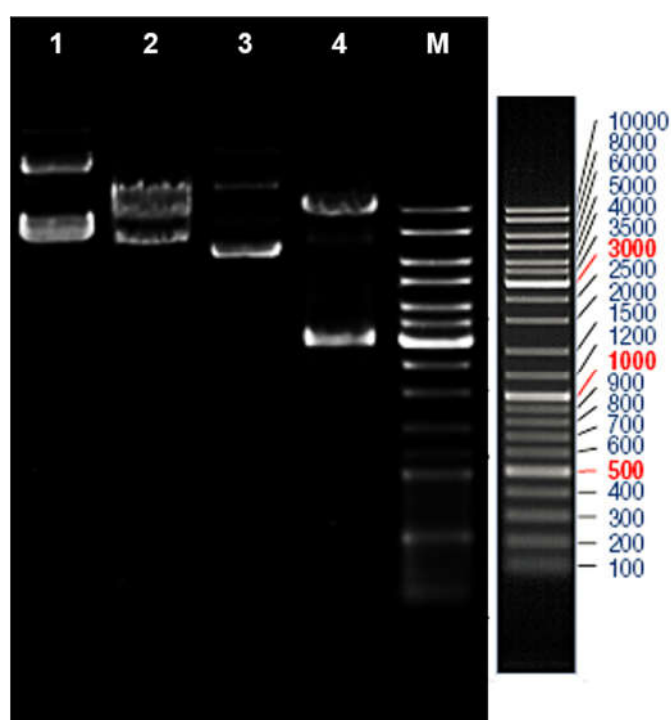


Figure 16. Characterisation of the parental plasmid-COL7A1 (PP-COL7A1) and minicircle-COL7A1 (MC-COL7A1) structure. Lane 1: undigested PP-COL7A1; Lane 2: PP-COL7A1 digested with *EcoR* I, the band above represents the COL7A1 gene (~8.9 kb); Lane 3: undigested MC-COL7A1; Lane 4: MC-COL7A1 digested with *EcoR* I, the band above represents the COL7A1 gene (~8.9 kb); M: standard DNA ladder.

3.2.2 Effect of Minicircle on Long-Term Expression of Type VII Collagen

Given the larger size of PP-COL7A1 DNA, it requires increased usage of Xfect™ reagent, which raise the level of cytotoxicity compared to the MC-COL7A1 vector. To achieve maximum restoration of C7 while maintaining minimal cytotoxicity, the same mass of the MC-COL7A1 and PP-COL7A1 vectors were utilised in this study for RDEBK cell transfections. DNA amount was defined as the highest quantity not resulting in any significant cytotoxic effects for PP-COL7A1 groups (data not shown). **Figure 17** indicates the reduction of RFP expression in both MC-COL7A1 and PP-COL7A1 groups over a two-week period. It was shown that RFP expression was slower than GFP as former described. Peak expression appeared during the days 6-9 depending on the different given treatments, and the MC-COL7A1 treated group showed significantly enhanced RFP expression compared to that of PP-COL7A1 throughout the entire experiment. At day 15, very weak fluorescence was detected for the PP-COL7A1 group, while the MC-COL7A1 group still showed a strong level of RFP expression. Type VII collagen is a cell secreted protein⁶, thus the culture supernatant was collected every three days and evaluated by western blotting assays. It is difficult to find a reliable loading control in this case, therefore harvested culture supernatants were concentrated, denatured and loaded onto polyacrylamide gels with equal amount of total protein between groups. Western blotting results indicated the significantly higher expression of C7 in the MC-COL7A1 compared to the PP-COL7A1 treatment (**Figure 18**), which was consistent with previous RFP fluorescence observations. For the first two time points, the MC-COL7A1 band's exposure was much stronger than the PP-COL7A1 band. Then the PP-COL7A1 band was barely visible on day 9, while the MC-COL7A1 treatment lasted for 15 days. Densitometry analysis of western blotting results was performed to quantify the treatment bands using ImageJ imaging software. These results further demonstrated that the MC-COL7A1 vectors significantly prolonged C7 expression (**Figure 18B**).

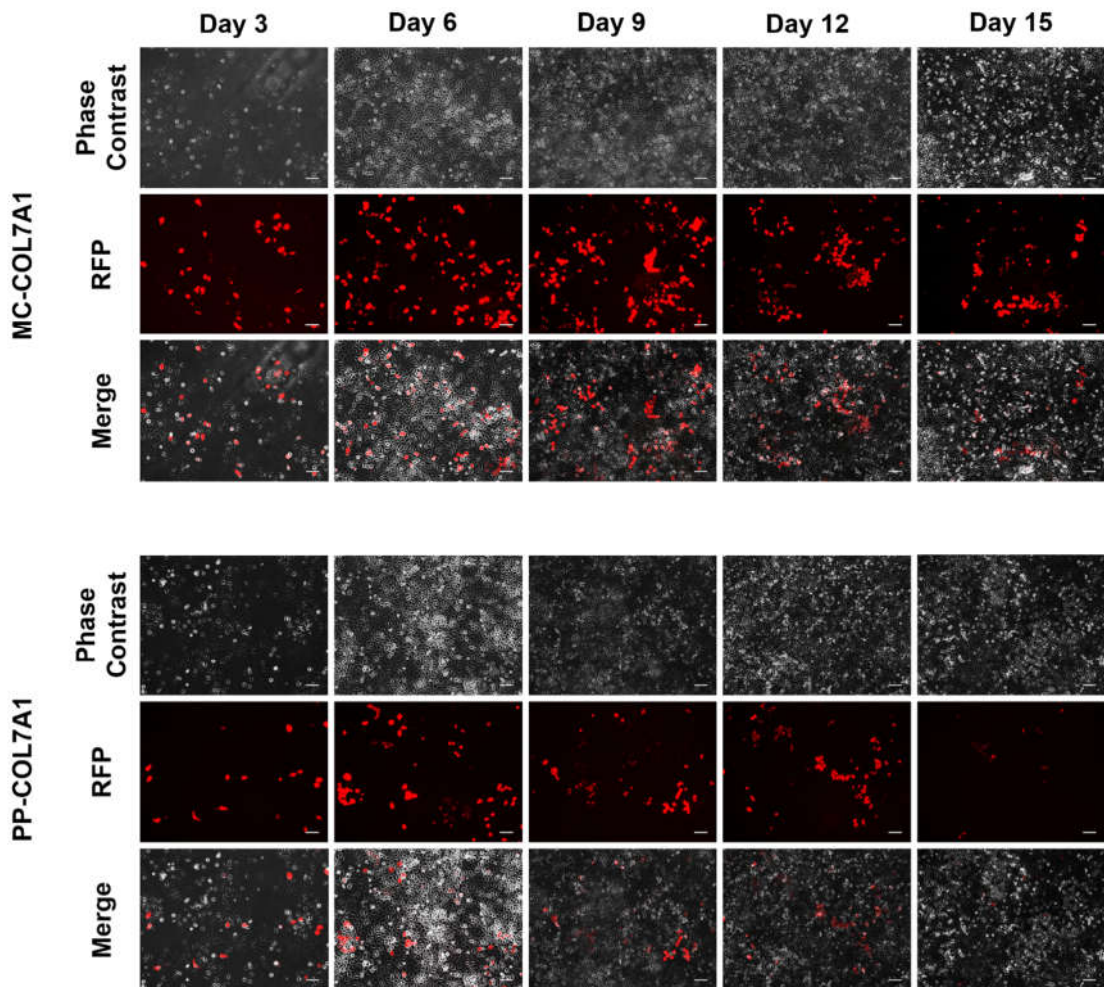


Figure 17. Representative images of red fluorescence expression on transfected RDEB keratinocytes (RDEBK) up to 15 days post MC-COL7A1 and PP-COL7A1 transfection. (Scale bars in all cases represent 100 μm).

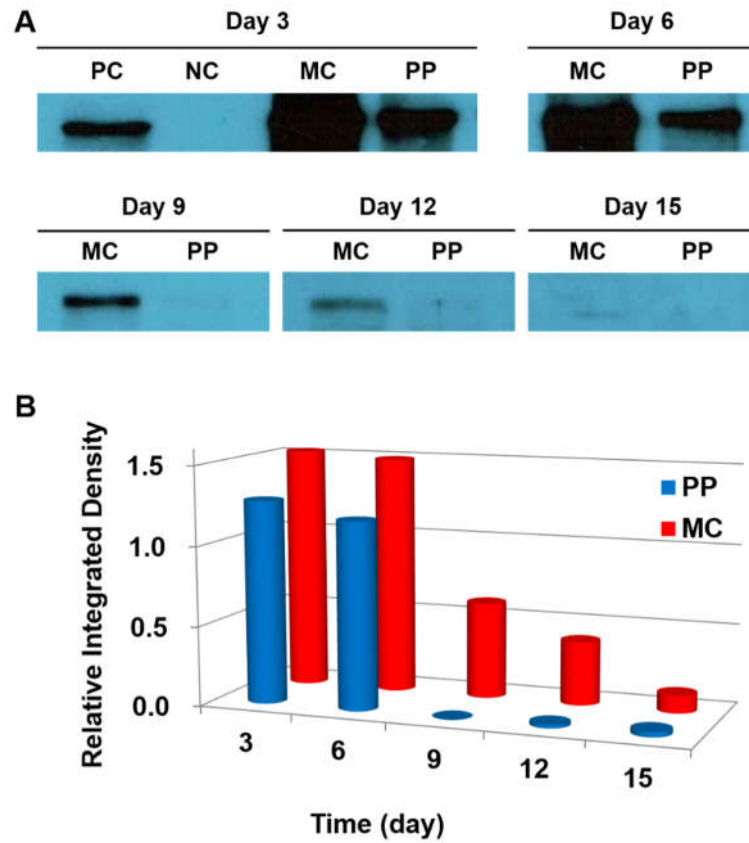


Figure 18. Western blotting results for concentrated supernatant harvested on 3 to 15 days post transfection. (A) Blotting results on exposure films; (B) Relative integrated density from western blotting results by ImageJ analysis, normalised by the density of PC band. PC: positive control of the supernatant from NHK culture; NC: negative control of the supernatant from non-transfected RDEBK cells.

Chapter Four

Conclusions and Future Directions

4.1 Conclusions

In summary, non-viral MC vectors with the COL7A1 gene were successfully built up. The MC gene vector without the bacterial backbone significantly increased the transfection efficiency and prolonged the expressing duration of the reporter transgene. Furthermore, long-term expression of type VII collagen in RDEBK was achieved by the transfection of MC-COL7A1 gene vector, which showed potential for a new application of non-viral delivery method on RDEB therapy.

4.2 Future Directions

Over the past decade, significant developments have been made in the treatment of RDEB. Patients are provided with a variety of hopeful treatments in the clinical trial rather than only palliative measures before. The optimal treatment of RDEB would eventually rely on the combination of multiple therapies, such as the autologous cells modification through gene therapy method following cell therapy implanting approach. The investigation of RDEB therapy also promotes the development of other genodermatosis.

In this thesis, preliminary *in vitro* study of MC application in RDEB therapy was performed. For the next step, *in vivo* systemic gene delivery is a targeting approach to deliver MC-COL7A1 for RDEB treatment, which may be achieved by introducing a tissue-specific promoter on transgene vector. The construction of MC system with tissue-specific promoter has been completed (See Appendix I). Future work will be focused on systemic delivery of tissue-specific MC-COL7A1 vector *in vivo*.

Additionally, the modification of MC structure can be considered to achieve a more

efficient system. For example, scaffold/matrix attachment regions (S/MAR) are sequences in eukaryotic chromosomes where the nuclear matrix attached, which are required for authentic and efficient chromosomal replication and transcription. With an affinity for the nuclear matrix, S/MAR sequences may mediate the delivering vector MC as maintenance elements in transfected cells to prolong the gene expression.

Further research should also be considered on the potential of safe, efficient non-viral gene delivery system. The results presented here are the pilot studies of the non-viral system to pave the way for future clinical therapies of genetic disorders.

References

1. Pearson RW. Clinicopathologic types of epidermolysis bullosa and their nondermatological complications. *Arch Dermatol*. 1988 May;124(5):718–25.
2. Perdoni C, Osborn MJ, Tolar J. Gene editing toward the use of autologous therapies in recessive dystrophic epidermolysis bullosa. *Transl Res*. 2016 Feb;168:50–8.
3. Fine JD, Bruckner-Tuderman L, Eady RAJ, Bauer EA, Bauer JW, Has C, et al. Inherited epidermolysis bullosa: Updated recommendations on diagnosis and classification. *J Am Acad Dermatol*. 2014 Jun;70(6):1103–26.
4. Epstein EH. The genetics of human skin diseases. *Curr Opin Genet Dev*. 1996 Jun;6(3):295–300.
5. Soro L, Bartus C, Purcell S. Recessive dystrophic epidermolysis bullosa: A review of disease pathogenesis and update on future therapies. *J Clin Aesthet Dermatol*. 2015 May;8(5):41–6.
6. Bruckner-Tuderman L, Höpfner B, Hammami-Hauasli N. Biology of anchoring fibrils: Lessons from dystrophic epidermolysis bullosa. *Matrix Biol*. 1999 Feb;18(1):43–54.
7. Bentz H, Morris NP, Murray LW, Sakai LY, Hollister DW, Burgeson RE. Isolation and partial characterization of a new human collagen with an extended triple-helical structural domain. *Proc Natl Acad Sci U S A*. 1983 Jun;80(11):3168–72.
8. Bruckner-Tuderman L, Rügger S, Odermatt B, Mitsuhashi Y, Schnyder UW. Lack of type VII collagen in unaffected skin of patients with severe recessive dystrophic epidermolysis bullosa. *Dermatology*. 1988;176(2):57–64.
9. Chung HJ, Uitto J. Type VII collagen: The anchoring fibril protein at fault in dystrophic epidermolysis bullosa. *Dermatol Clin*. 2010 Jan;28(1):93–105.
10. Ferrari S, Pellegrini G, Mavilio F, De Luca M. Gene therapy approaches for epidermolysis bullosa. *Clin Dermatol*. 2005;23(4):430–6.
11. Järvikallio A, Pulkkinen L, Uitto J. Molecular basis of dystrophic epidermolysis bullosa: Mutations in the type VII collagen gene (COL7A1). *Hum Mutat*. 1997;10(5):338–47.
12. Dang N, Murrell DF. Mutation analysis and characterization of COL7A1 mutations in dystrophic epidermolysis bullosa. *Exp Dermatol*. 2008 Jul;17(7):553–68.

13. Martins VL, Vyas JJ, Chen M, Purdie K, Mein CA, South AP, et al. Increased invasive behaviour in cutaneous squamous cell carcinoma with loss of basement-membrane type VII collagen. *J Cell Sci.* 2009;122(11):1788–99.
14. Abdul-Wahab A, Qasim W, McGrath JA. Gene therapies for inherited skin disorders. *Semin Cutan Med Surg.* 2014 Jun;33(2):83–90.
15. Fine J-D, Johnson LB, Weiner M, Li K-P, Suchindran C. Epidermolysis bullosa and the risk of life-threatening cancers: the National EB Registry experience, 1986-2006. *J Am Acad Dermatol.* 2009 Feb;60(2):203–11.
16. Fine J-D, Hintner H. *Life with epidermolysis bullosa (EB): Etiology, diagnosis, multidisciplinary care and therapy.* Springer Vienna; 2009.
17. Hubbard LD, Mayre-Chilton K. Quality of life among adults with epidermolysis bullosa living with a gastrostomy tube since childhood. *Qual Health Res.* 2015 Mar;25(3):310–9.
18. Woodley DT, Keene DR, Atha T, Huang Y, Lipman K, Li W, et al. Injection of recombinant human type VII collagen restores collagen function in dystrophic epidermolysis bullosa. *Nat Med.* 2004 Jul;10(7):693–5.
19. Remington J, Wang X, Hou Y, Zhou H, Burnett J, Muirhead T, et al. Injection of recombinant human type VII collagen corrects the disease phenotype in a murine model of dystrophic epidermolysis bullosa. *Mol Ther.* 2009 Jan;17(1):26–33.
20. Woodley DT, Wang X, Amir M, Hwang B, Remington J, Hou Y, et al. Intravenously injected recombinant human type VII collagen homes to skin wounds and restores skin integrity of dystrophic epidermolysis bullosa. *J Invest Dermatol.* 2013 Jul;133(7):1910–3.
21. Bruckner-Tuderman L. Can type VII collagen injections cure dystrophic epidermolysis bullosa? *Mol Ther.* 2009 Jan;17(1):6–7.
22. McGrath JA, Ishida-Yamamoto A, O’Grady A, Leigh IM, Eady RAJ. Structural variations in anchoring fibrils in dystrophic epidermolysis bullosa: Correlation with type VII collagen expression. *J Invest Dermatol.* 1993 Apr;100(4):366–72.
23. Sawamura D, Nakano H, Matsuzaki Y. Overview of epidermolysis bullosa. *J Dermatol.* 2010 Mar;37(3):214–9.
24. Ortiz-Urda S, Lin Q, Green CL, Keene DR, Marinkovich MP, Khavari PA. Injection of genetically engineered fibroblasts corrects regenerated human epidermolysis bullosa skin tissue. *J Clin Invest.* 2003 Jan;111(2):251–5.
25. Wong T, Gammon L, Liu L, Mellerio JE, Dopping-Hepenstal PJC, Pacy J, et al. Potential of fibroblast cell therapy for recessive dystrophic epidermolysis bullosa.

- J Invest Dermatol. 2008 Sep;128(9):2179–89.
26. Nagy N, Almaani N, Tanaka A, Lai-Cheong JE, Techanukul T, Mellerio JE, et al. HB-EGF induces COL7A1 expression in keratinocytes and fibroblasts: Possible mechanism underlying allogeneic fibroblast therapy in recessive dystrophic epidermolysis Bullosa. *J Invest Dermatol.* 2011 Aug;131(8):1771–4.
 27. Petrof G, Martinez-Queipo M, Mellerio JE, Kemp P, McGrath JA. Fibroblast cell therapy enhances initial healing in recessive dystrophic epidermolysis bullosa wounds: Results of a randomized, vehicle-controlled trial. *Br J Dermatol.* 2013 Nov;169(5):1025–33.
 28. Woodley DT, Krueger GG, Jorgensen CM, Fairley JA, Atha T, Huang Y, et al. Normal and gene-corrected dystrophic epidermolysis bullosa fibroblasts alone can produce type VII collagen at the basement membrane zone. *J Invest Dermatol.* 2003 Nov;121(5):1021–8.
 29. Woodley DT, Remington J, Huang Y, Hou Y, Li W, Keene DR, et al. Intravenously injected human fibroblasts home to skin wounds, deliver type VII collagen, and promote wound healing. *Mol Ther.* 2007 Mar;15(3):628–35.
 30. Branski LK, Gauglitz GG, Herndon DN, Jeschke MG. A review of gene and stem cell therapy in cutaneous wound healing. *Burns.* 2009 Mar;35(2):171–80.
 31. Chino T, Tamai K, Yamazaki T, Otsuru S, Kikuchi Y, Nimura K, et al. Bone marrow cell transfer into fetal circulation can ameliorate genetic skin diseases by providing fibroblasts to the skin and inducing immune tolerance. *Am J Pathol.* 2008 Sep;173(3):803–14.
 32. Tolar J, Ishida-Yamamoto A, Riddle M, McElmurry RT, Osborn M, Xia L, et al. Amelioration of epidermolysis bullosa by transfer of wild-type bone marrow cells. *Blood.* 2009 Jan;113(5):1167–74.
 33. Wagner JE, Ishida-Yamamoto A, McGrath JA, Hordinsky M, Keene DR, Woodley DT, et al. Bone marrow transplantation for recessive dystrophic epidermolysis bullosa. *N Engl J Med.* 2010 Aug;363(7):629–39.
 34. Kiuru M, Itoh M, Cairo MS, Christiano AM. Bone marrow stem cell therapy for recessive dystrophic epidermolysis bullosa. *Dermatol Clin.* 2010;28(2):371–82.
 35. Geyer MB, Radhakrishnan K, Giller R, Umegaki N, Harel S, Kiuru M, et al. Reduced toxicity conditioning and allogeneic hematopoietic progenitor cell transplantation for recessive dystrophic epidermolysis bullosa. *J Pediatr.* 2015;167(3):765–9.
 36. Tolar J, Wagner JE. Management of severe epidermolysis bullosa by haematopoietic transplant: Principles, perspectives and pitfalls. *Exp Dermatol.* 2012 Dec;21(12):896–900.

37. Alexeev V, Uitto J, Igoucheva O. Gene expression signatures of mouse bone marrow-derived mesenchymal stem cells in the cutaneous environment and therapeutic implications for blistering skin disorder. *Cytotherapy*. 2011 Jan;13(1):30–45.
38. Conget P, Rodriguez F, Kramer S, Allers C, Simon V, Palisson F, et al. Replenishment of type VII collagen and re-epithelialization of chronically ulcerated skin after intradermal administration of allogeneic mesenchymal stromal cells in two patients with recessive dystrophic epidermolysis bullosa. *Cytotherapy*. 2010;12(3):429–31.
39. Petrof G, Lwin SM, Martinez-Queipo M, Abdul-Wahab A, Tso S, Mellerio JE, et al. Potential of systemic allogeneic mesenchymal stromal cell therapy for children with recessive dystrophic epidermolysis bullosa. *J Invest Dermatol*. 2015;135(9):2319–21.
40. Zarrabi M, Mousavi SH, Abroun S, Sadeghi B. Potential uses for cord blood mesenchymal stem cells. *Cell J*. 2014;15(4):274–81.
41. Luo G, Cheng W, He W, Wang X, Tan J, Fitzgerald M, et al. Promotion of cutaneous wound healing by local application of mesenchymal stem cells derived from human umbilical cord blood. *Wound Repair Regen*. 2010;18(5):506–13.
42. Kim YS, Ahn Y, Kwon JS, Cho YK, Jeong MH, Cho JG, et al. Priming of mesenchymal stem cells with oxytocin enhances the cardiac repair in ischemia/reperfusion injury. *Cells Tissues Organs*. 2012;195(5):428–42.
43. De Luca M, Pellegrini G, Mavilio F. Gene therapy of inherited skin adhesion disorders: a critical overview. *Br J Dermatol*. 2009 Jul;161(1):19–24.
44. Takahashi K, Yamanaka S. Induction of pluripotent stem cells from mouse embryonic and adult fibroblast cultures by defined factors. *Cell*. 2006 Aug;126(4):663–76.
45. Takahashi K, Tanabe K, Ohnuki M, Narita M, Ichisaka T, Tomoda K, et al. Induction of pluripotent stem cells from adult human fibroblasts by defined factors. *Cell*. 2007 Nov;131(5):861–72.
46. Tolar J, Xia L, Riddle MJ, Lees CJ, Eide CR, McElmurry RT, et al. Induced pluripotent stem cells from individuals with recessive dystrophic epidermolysis bullosa. *J Invest Dermatol*. 2011;131(4):848–56.
47. Sebastiano V, Zhen HH, Haddad B, Derafshi BH, Bashkirova E, Melo SP, et al. Human COL7A1-corrected induced pluripotent stem cells for the treatment of recessive dystrophic epidermolysis bullosa. *Sci Transl Med*. 2014 Nov;6(264):264ra163.

48. Wenzel D, Bayerl J, Nyström A, Bruckner-Tuderman L, Meixner A, Penninger JM. Genetically corrected iPSCs as cell therapy for recessive dystrophic epidermolysis bullosa. *Sci Transl Med*. 2014 Nov;6(264):264ra165.
49. Ma H, Morey R, O'Neil RC, He Y, Daughtry B, Schultz MD, et al. Abnormalities in human pluripotent cells due to reprogramming mechanisms. *Nature*. 2014;511(7508):177–83.
50. Ibraheem D, Elaissari A, Fessi H. Gene therapy and DNA delivery systems. *Int J Pharm*. 2014;459(1):70–83.
51. Davies JC, Geddes DM, Alton EW. Gene therapy for cystic fibrosis. *J Gene Med*. 2001;3(5):409–17.
52. Rochlitz CF. Gene therapy of cancer. *Swiss Med Wkly*. 2001;131:4–9.
53. Yu M, Poeschla E, Wong-Staal F. Progress towards gene therapy for HIV infection. *Gene Ther*. 1994;1(1):13–26.
54. Dishart KL, Work LM, Denby L, Baker AH. Gene therapy for cardiovascular disease. *J Biomed Biotechnol*. 2003;2003(2):138–48.
55. Kohn DB, Sadelain M, Glorioso JC. Occurrence of leukaemia following gene therapy of X-linked SCID. *Nat Rev Cancer*. 2003 Jul;3(7):477–88.
56. Wang W, Li W, Ma N, Steinhoff G. Non-viral gene delivery methods. *Curr Pharm Biotechnol*. 2013;14(1):46–60.
57. Gardlík R, Pálffy R, Hodosy J, Lukács J, Turna J, Celec P. Vectors and delivery systems in gene therapy. *Med Sci Monit*. 2005;11(4):RA110-21.
58. Chen M, O'Toole EA, Muellenhoff M, Medina E, Kasahara N, Woodley DT. Development and characterization of a recombinant truncated type VII collagen “minigene”. Implication for gene therapy of dystrophic epidermolysis bullosa. *J Biol Chem*. 2000 Aug;275(32):24429–35.
59. Chen M, Kasahara N, Keene DR, Chan L, Hoeffler WK, Finlay D, et al. Restoration of type VII collagen expression and function in dystrophic epidermolysis bullosa. *Nat Genet*. 2002 Dec;32(4):670–5.
60. Baldeschi C, Gache Y, Rattenholl A, Bouillé P, Danos O, Ortonne JP, et al. Genetic correction of canine dystrophic epidermolysis bullosa mediated by retroviral vectors. *Hum Mol Genet*. 2003;12(15):1897–905.
61. Gache Y, Baldeschi C, Del Rio M, Gagnoux-Palacios L, Larcher F, Lacour J, et al. Construction of skin equivalents for gene therapy of recessive dystrophic epidermolysis bullosa. *Hum Gene Ther*. 2004 Oct;15(10):921–33.
62. Titeux M, Pendaries V, Zanta-Boussif MA, Décha A, Pironon N, Tonasso L, et

- al. SIN retroviral vectors expressing COL7A1 under human promoters for ex vivo gene therapy of recessive dystrophic epidermolysis bullosa. *Mol Ther.* 2010;18(8):1509–18.
63. Sawamura D, Yasukawa K, Kodama K, Yokota K, Sato-Matsumura KC, Toshihiro T, et al. The majority of keratinocytes incorporate intradermally injected plasmid DNA regardless of size but only a small proportion of cells can express the gene product. *J Invest Dermatol.* 2002 Jun;118(6):967–71.
 64. Mecklenbeck S, Compton SH, Mejía JE, Cervini R, Hovnanian A, Bruckner-Tuderman L, et al. A microinjected COL7A1-PAC vector restores synthesis of intact procollagen VII in a dystrophic epidermolysis bullosa keratinocyte cell line. *Hum Gene Ther.* 2002 Sep;13(13):1655–62.
 65. Ortiz-Urda S, Thyagarajan B, Keene DR, Lin Q, Fang M, Calos MP, et al. Stable nonviral genetic correction of inherited human skin disease. *Nat Med.* 2002;8(10):1166–70.
 66. Šimčíková M, Prather KLJ, Prazeres DMF, Monteiro GA. Towards effective non-viral gene delivery vector. *Biotechnol Genet Eng Rev.* 2015;31(1–2):82–107.
 67. Ferraro B, Morrow MP, Hutnick NA, Shin TH, Lucke CE, Weiner DB. Clinical applications of DNA vaccines: Current progress. *Clin Infect Dis.* 2011 Aug;53(3):296–302.
 68. Lara AR, Ramírez OT. Plasmid DNA production for therapeutic applications. In: Lorence A, editor. *Recombinant gene expression.* Totowa, NJ: Humana Press; 2012. p. 271–303.
 69. Williams JA, Carnes AE, Hodgson CP. Plasmid DNA vaccine vector design: Impact on efficacy, safety and upstream production. *Biotechnol Adv.* 2009;27(4):353–70.
 70. Kushner PJ, Baxter JD, Duncan KG, Lopez GN, Schaufele F, Uht RM, et al. Eukaryotic regulatory elements lurking in plasmid DNA: the activator protein-1 site in pUC. *Mol Endocrinol.* 1994;8(4):405–7.
 71. Peterson DO, Beifuss KK, Morley KL. Context-dependent gene expression: cis-acting negative effects of specific procaryotic plasmid sequences on eucaryotic genes. *Mol Cell Biol.* 1987;7(4):1563–7.
 72. Soubrier F, Cameron B, Manse B, Somarriba S, Dubertret C, Jaslin G, et al. pCOR: a new design of plasmid vectors for nonviral gene therapy. *Gene Ther.* 1999 Aug;6(8):1482–8.
 73. Williams SG, Cranenburgh RM, Weiss AME, Wrighton CJ, Sherratt DJ, Hanak JAJ. Repressor titration: A novel system for selection and stable maintenance of recombinant plasmids. *Nucleic Acids Res.* 1998;26(9):2120–4.

74. Cranenburgh RM, Hanak JA, Williams SG, Sherratt DJ. Escherichia coli strains that allow antibiotic-free plasmid selection and maintenance by repressor titration. *Nucleic Acids Res.* 2001;29(5):e26.
75. Szpirer CY, Milinkovitch MC. Separate-component-stabilization system for protein and DNA production without the use of antibiotics. *Biotechniques.* 2005 May;38(5):775–81.
76. Mairhofer J, Pfaffenzeller I, Merz D, Grabherr R. A novel antibiotic free plasmid selection system: Advances in safe and efficient DNA therapy. *Biotechnol J.* 2008 Jan;3(1):83–9.
77. Luke J, Carnes AE, Hodgson CP, Williams JA. Improved antibiotic-free DNA vaccine vectors utilizing a novel RNA based plasmid selection system. *Vaccine.* 2009;27(46):6454–9.
78. Valera A, Perales JC, Hatzoglou M, Bosch F. Expression of the neomycin-resistance (neo) gene induces alterations in gene expression and metabolism. *Hum Gene Ther.* 1994;5(4):449–56.
79. Oliveira PH, Mairhofer J. Marker-free plasmids for biotechnological applications - implications and perspectives. *Trends Biotechnol.* 2013;31(9):539–47.
80. Prather KJ, Sagar S, Murphy J, Chartrain M. Industrial scale production of plasmid DNA for vaccine and gene therapy: Plasmid design, production, and purification. *Enzyme Microb Technol.* 2003;33(7):865–83.
81. Boshart M, Weber F, Jahn G, Dorsch-Häsler K, Fleckenstein B, Schaffner W. A very strong enhancer is located upstream of an immediate early gene of human cytomegalovirus. *Cell.* 1985;41(2):521–30.
82. Kutzler MA, Weiner DB. DNA vaccines: ready for prime time? *Nat Rev Genet.* 2008;9(10):776–88.
83. André S, Seed B, Eberle J, Schraut W, Bültmann A, Haas J. Increased immune response elicited by DNA vaccination with a synthetic gp120 sequence with optimized codon usage. *J Virol.* 1998;72(2):1497–503.
84. Cashman KA, Broderick KE, Wilkinson ER, Shaia CI, Bell TM, Shurtleff AC, et al. Enhanced efficacy of a codon-optimized DNA vaccine encoding the glycoprotein precursor gene of lassa virus in a guinea pig disease model when delivered by dermal electroporation. *Vaccines.* 2013;1(3):262–77.
85. Hunt AG, Xu R, Addepalli B, Rao S, Forbes KP, Meeks LR, et al. Arabidopsis mRNA polyadenylation machinery: Comprehensive analysis of protein-protein interactions and gene expression profiling. *BMC Genomics.* 2008;9:220.
86. Proudfoot NJ. Ending the message: Poly(A) signals then and now. *Genes Dev.*

- 2011;25(17):1770–82.
87. Guhaniyogi J, Brewer G. Regulation of mRNA stability in mammalian cells. *Gene*. 2001;265(1–2):11–23.
 88. Catanese DJ, Fogg JM, Schrock DE, Gilbert BE, Zechiedrich L. Supercoiled minivector DNA resists shear forces associated with gene therapy delivery. *Gene Ther*. 2012;19(1):94–100.
 89. Chen ZY, He CY, Meuse L, Kay MA. Silencing of episomal transgene expression by plasmid bacterial DNA elements in vivo. *Gene Ther*. 2004;11(10):856–64.
 90. Darquet AM, Cameron B, Wils P, Scherman D, Crouzet J. A new DNA vehicle for nonviral gene delivery: supercoiled minicircle. *Gene Ther*. 1997;4(12):1341–9.
 91. Landy A. Dynamic, structural, and regulatory aspects of lambda site-specific recombination. *Annu Rev Biochem*. 1989;58(1):913–41.
 92. Kreiss P, Cameron B, Darquet AM, Scherman D, Crouzet J. Production of a new DNA vehicle for gene transfer using site-specific recombination. *Appl Microbiol Biotechnol*. 1998 May;49(5):560–7.
 93. Bigger BW, Tolmachov O, Collombet JM, Fragkos M, Palaszewski I, Coutelle C. An araC-controlled bacterial cre expression system to produce DNA minicircle vectors for nuclear and mitochondrial gene therapy. *J Biol Chem*. 2001 Jun;276(25):23018–27.
 94. Chen ZY, He CY, Ehrhardt A, Kay MA. Minicircle DNA vectors devoid of bacterial DNA result in persistent and high-level transgene expression in vivo. *Mol Ther*. 2003;8(3):495–500.
 95. Mayrhofer P, Blaesens M, Schlee M, Jechlinger W. Minicircle-DNA production by site specific recombination and protein-DNA interaction chromatography. *J Gene Med*. 2008;10(11):1253–69.
 96. Chen ZY, He CY, Kay MA. Improved production and purification of minicircle DNA vector free of plasmid bacterial sequences and capable of persistent transgene expression in vivo. *Hum Gene Ther*. 2005;16(1):126–31.
 97. Kay MA, He CY, Chen ZY. A robust system for production of minicircle DNA vectors. *Nat Biotechnol*. 2010 Dec;28(12):1287–9.
 98. Canatella PJ, Prausnitz MR. Prediction and optimization of gene transfection and drug delivery by electroporation. *Gene Ther*. 2001;8(19):1464–9.
 99. Daud AI, DeConti RC, Andrews S, Urbas P, Riker AI, Sondak VK, et al. Phase I trial of interleukin-12 plasmid electroporation in patients with metastatic

- melanoma. *J Clin Oncol*. 2008 Dec;26(36):5896–903.
100. Endoh M, Koibuchi N, Sato M, Morishita R, Kanzaki T, Murata Y, et al. Fetal gene transfer by intrauterine injection with microbubble-enhanced ultrasound. *Mol Ther*. 2002 May;5(5):501–8.
 101. Sheyn D, Kimelman-Bleich N, Pelled G, Zilberman Y, Gazit D, Gazit Z. Ultrasound-based nonviral gene delivery induces bone formation in vivo. *Gene Ther*. 2008;15:257–66.
 102. Zhang G, Song YK, Liu D. Long-term expression of human alpha1-antitrypsin gene in mouse liver achieved by intravenous administration of plasmid DNA using a hydrodynamics-based procedure. *Gene Ther*. 2000;7(15):1344–9.
 103. Fabre JW, Grehan A, Whitehorne M, Sawyer GJ, Dong X, Salehi S, et al. Hydrodynamic gene delivery to the pig liver via an isolated segment of the inferior vena cava. *Gene Ther*. 2008;15(6):452–62.
 104. Klein TM, Wolf ED, Wu R, Sanford JC. High-velocity microprojectiles for delivering nucleic acids into living cells. *Nature*. 1987 May;327(6117):70–3.
 105. O'Brien J, Lummis SCR. An improved method of preparing microcarriers for biolistic transfection. *Brain Res Protoc*. 2002;10(1):12–5.
 106. Yin H, Kanasty RL, Eltoukhy AA, Vegas AJ, Dorkin JR, Anderson DG. Non-viral vectors for gene-based therapy. *Nat Rev Genet*. 2014;15(8):541–55.
 107. Zuhorn IS, Engberts JBFN, Hoekstra D. Gene delivery by cationic lipid vectors: Overcoming cellular barriers. *Eur Biophys J*. 2007;36(4):349–62.
 108. Thomas M, Klibanov AM. Non-viral gene therapy: Polycation-mediated DNA delivery. *Appl Microbiol Biotechnol*. 2003;62(1):27–34.
 109. Discher DE, Ahmed F. Polymersomes. *Annu Rev Biomed Eng*. 2006;8:323–41.
 110. Martin ME, Rice KG. Peptide-guided gene delivery. *AAPS J*. 2007;9(1):E18-29.
 111. Sokolova V, Epple M. Inorganic nanoparticles as carriers of nucleic acids into cells. *Angew Chemie Int Ed*. 2008;47(8):1382–95.
 112. Gao X, Kim K-S, Liu D. Nonviral gene delivery: What we know and what is next. *AAPS J*. 2007;9(1):E92–104.
 113. Rynnänen J, Sollberg S, Parente MG, Chung LC, Christiano AM, Uitto J. Type VII collagen gene expression by cultured human cells and in fetal skin. Abundant mRNA and protein levels in epidermal keratinocytes. *J Clin Invest*. 1992;89(1):163–8.
 114. Hovnanian A, Rochat A, Bodemer C, Petit E, Rivers CA, Prost C, et al. Characterization of 18 new mutations in COL7A1 in recessive dystrophic

- epidermolysis bullosa provides evidence for distinct molecular mechanisms underlying defective anchoring fibril formation. *Am J Hum Genet.* 1997 Sep;61(3):599–610.
115. Chamorro C, Almarza D, Duarte B, Llamas SG, Murillas R, García M, et al. Keratinocyte cell lines derived from severe generalized recessive epidermolysis bullosa patients carrying a highly recurrent COL7A1 homozygous mutation: Models to assess cell and gene therapies in vitro and in vivo. *Exp Dermatol.* 2013;22(9):601–3.
 116. Zheng C, Baum B. Evaluation of promoters for use in tissue-specific gene delivery. In: LeDoux JM, editor. *Gene therapy protocols: design and characterization of gene transfer vectors.* Totowa, NJ: Humana Press; 2008. p. 205–19.
 117. Osborn MJ, McElmurry RT, Lees CJ, DeFeo AP, Chen Z-Y, Kay MA, et al. Minicircle DNA-based gene therapy coupled with immune modulation permits long-term expression of α -L-iduronidase in mice with mucopolysaccharidosis type I. *Mol Ther.* 2011;19(3):450–60.
 118. Verrecchia F, Vindevoghel L, Lechleider RJ, Uitto J, Roberts AB, Mauviel A. Smad3/AP-1 interactions control transcriptional responses to TGF- β in a promoter-specific manner. *Oncogene.* 2001;20(26):3332–40.
 119. Pendaries V, Verrecchia F, Michel S, Mauviel A. Retinoic acid receptors interfere with the TGF-beta/Smad signaling pathway in a ligand-specific manner. *Oncogene.* 2003;22(50):8212–20.

Appendix I

Construction of Minicircle-COL7A1 with Tissue-Specific Promoter

In non-viral vectors for gene therapy, the expression cassette includes three main components: promoter, the therapeutic gene (gene of interest) and polyadenylation signal⁶⁶. The commonly used promoters are mostly based on a virus, which can control the expression of the therapeutic gene in mammalian cells⁶⁶. As each gene has its own promoter in mammalian cells and some tissue-specific promoters can only be activated in a certain cell type¹¹⁶, the use of tissue-specific promoter can reduce off-target gene expression and enhance the persistent gene expression in targeted tissue. The substitution of the virus-based promoter by host tissue-specific promoter can also decrease its immune response. Osborn et al. developed a minicircle vector combined with the liver-specific promoter and microRNA target sequences for the treatment of mucopolysaccharidosis type I (MPS I), a α -L-iduronidase (IDUA) gene mutation disease¹¹⁷. The insertion of liver-specific promoter enhanced the liver expression level of IDUA for nearly ten times higher than other organs *in vivo*, but not for long-term expression. The addition of mirT sequences helped prolong the gene expression period up to 80 days¹¹⁷. Given the further investigation for systemic delivery of transgene vectors *in vivo*, the transgene should be expressed in the desired cell type, i.e. cutaneous cells for type VII collagen expression. By using tissue-specific promoters, it can diminish the immune rejection and inhibit the silencing of the transgene. Here, to further improve the MC-COL7A1 system, the virus-based CMV promoter was substituted by a human-derived COL7A1 promoter, which targeted the C7 expression in specific cell types^{62,118,119}.

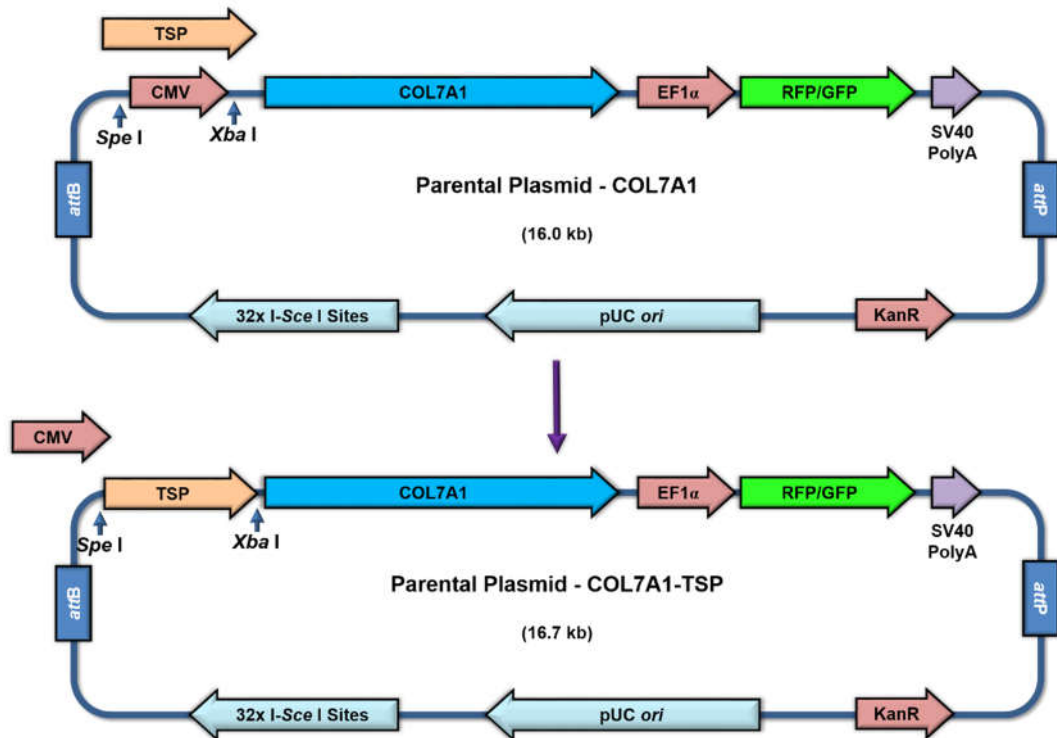


Figure i. Schematic representation of exchanging the CMV promoter driving COL7A1 gene to a tissue-specific promoter.

The COL7A1 promoter gene was preserved in a pEX-K backbone. Similar to the construction procedures of PP-COL7A1 and MC-COL7A1, the MN511/MN511-COL7A1 vector and COL7A1 promoter were both digested by *Spe* I and *Xba* I restriction enzyme and ligated using T4 Ligase. Here, low DNA extraction efficiency of the large fragments (COL7A1) was compensated by increasing the digested plasmid amount and advanced gel extraction kits QIAEX II®.

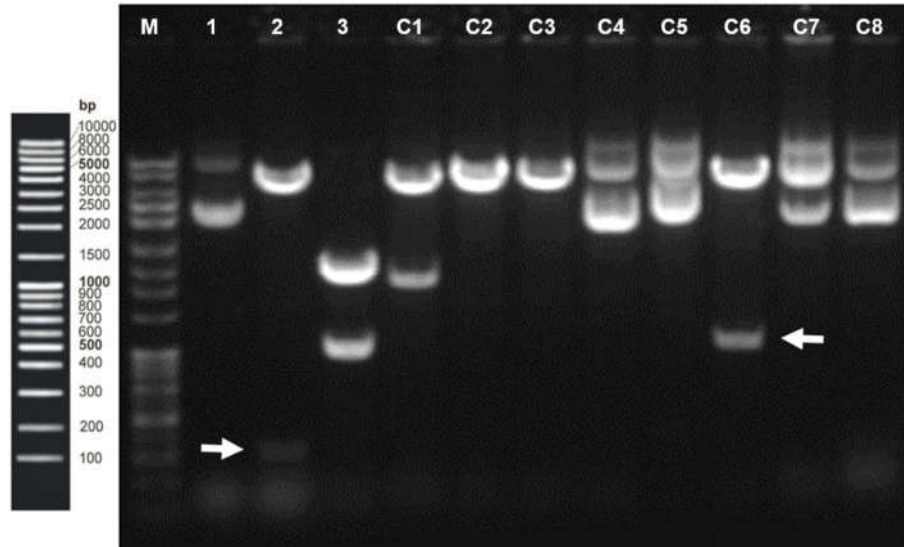


Figure ii. Verification of screened positive colonies in MN511/TSP construction.

Lane 1: undigested MN511 PP vector; Lane 2: PP vector digested by *Spe* I and *Xba* I, the band below represents the CMV promoter (~350 bp) as the right arrow shown; Lane 3: pEX-K/TSP vector digested by *Spe* I and *Xba* I, the lower band represents the TSP gene (~1.1 kb); C1-C8: ligated vectors digested by *Spe* I and *Xba* I from selected colonies No.1-8, respectively; M: standard DNA ladder. On C6 the lower band represents the same size as TSP contrast as the left arrow shown.

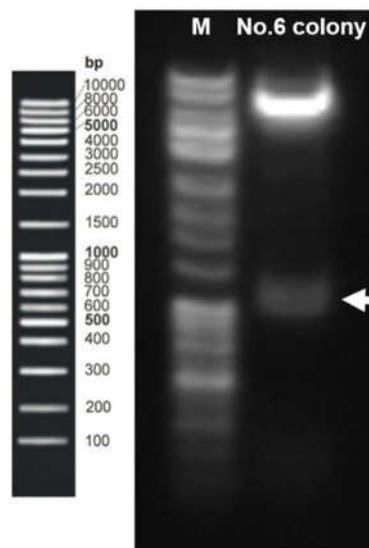


Figure iii. Confirmation of No. 6 colony in MN511/TSP construction. The bands of digested No. 6 vector presents the correct sizes. The arrow shows the TSP band.

As **Figure ii** shown, original supercoiled MN511 vector is presented in Lane 1, with a smaller displayed size due to the supercoiled structure. In Lane 2, the upper band represents the linearised MN511 vector devoid of CMV promoter, digested by *Spe* I and *Xba* I, while the lower band is the CMV promoter. In Lane 3, pEX-K/TSP plasmid was digested by *Spe* I and *Xba* I enzyme, in which the lower band indicates the COL7A1 promoter. Lane C1-C8 show the samples from chosen positive colonies digested by *Spe* I and *Xba* I. Correct digested fragments have been shown in Lane C6 (No. 6 colony), including an MN511 vector band (without CMV) and a COL7A1 promoter band, which demonstrated the success of MN511/TSP vector construction. A repeated confirmation was made on the vector in No. 6 colony, indicating the right size of two fragments at ~7 kb and ~1 kb (**Figure iii**).

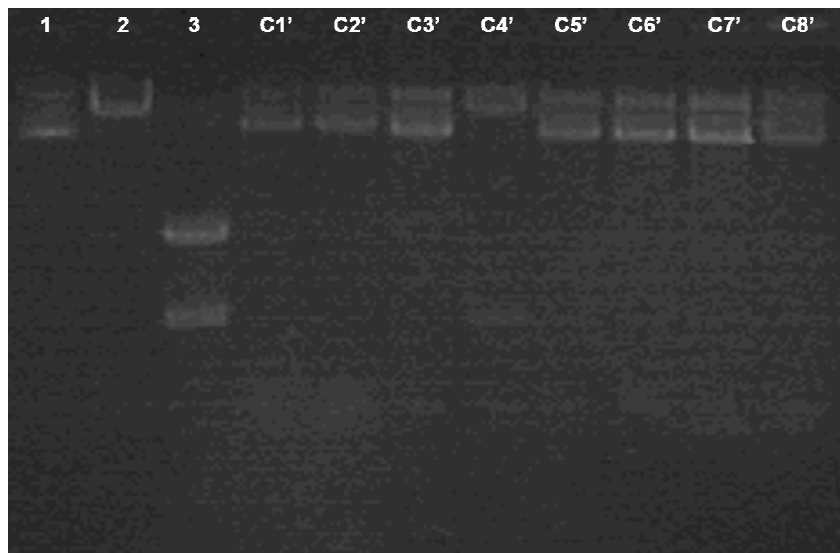


Figure iv. Verification of screened positive colonies in MN511-COL7A1/TSP construction. Lane 1: undigested PP-COL7A1 vector; Lane 2: PP-COL7A1 vector digested by *Spe* I and *Xba* I, the band above represents the linear vector without CMV promoter; Lane 3: pEX-K/TSP vector digested by *Spe* I and *Xba* I, the lower band represents the TSP gene; C1'-C8': ligated vectors digested by *Spe* I and *Xba* I from selected colonies No.1'-8', respectively. On C4' the upper band represents the same size as linear PP-COL7A1 vector without promoter.

For the construction of MN511COL7A1/TSP vector, a similar procedure was applied. In **Figure iv**, it is visible that all the upper bands of digested DNA from screened positive colonies are the same size as the undigested MN511-COL7A1 plasmid (Lane 1), except in Lane C4'. The upper band in Lane C4' represents the linearised MN511-COL7A1 fragments without CMV promoter as the upper band in Lane 2 shown, which reveals possibly correct constructed colony.

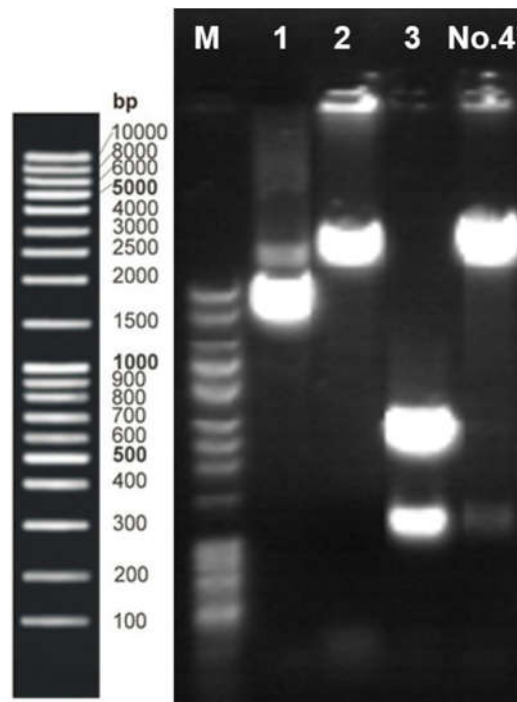


Figure v. Confirmation of No. 4' colony in MN511-COL7A1/TSP construction. The bands of digested No. 4' vector presents the correct sizes. Lane 1: undigested PP-COL7A1 vector; Lane 2: PP-COL7A1 vector digested by *Spe* I and *Xba* I, the band above represents the linear vector without CMV promoter; Lane 3: pEX-K/TSP vector digested by *Spe* I and *Xba* I, the lower band represents the TSP gene. The bands of digested No. 4' vector presents the correct sizes.

Repeated verification was made for the plasmid preserved in No. 4' colony by DNA electrophoresis. The digested No. 4' plasmid indicates two bands (**Figure v**, Lane No. 4'), which represent the right size of MN511-COL7A1 (without CMV) fragment (upper

band) and the TSP promoter fragment (lower band). Herein, it proved that the MN511-COL7A1/TSP vector was successfully constructed. The MN511/TSP and MN511-COL7A1/TSP vector construction results were further confirmed by sequencing and proved correct ligation.

Appendix II

Materials and Protocols

A. Materials and Reagents

Material	Supplier
BD ACCURI C6 flow cytometer	BD Biosciences
Electrophoresis chamber	Bio-rad
Power supply	
Lipofectamine® 2000 reagent	Bio-Sciences
rabbit anti-human type VII collagen poly-antibody	Calbiochem
anti-rabbit IgG with HRP-linked	Cell Signaling Technology
Xfect™ Transfection Reagent	Clontech
6X Sample Loading Buffer	Fisher Scientific
DNA ladder standard	
Ethylenediaminetetraacetic acid	Fluka
Propidium Iodide ReadyProbes® Reagent	Life technologies
Amicon® Ultra-15 Centrifugal Filter Units	Merck Millipore
CutSmart™ Buffer	New England Biolabs
<i>EcoR</i> I	
OLYMPUS-X41 microscope	Olympus
Partec CellTics® 50µm filter	Partec
T4 DNA Ligase & buffer	Promega
Keratinocyte Basal Medium	PromoCell
PromoCell kits	
QIAEX II® Gel Extraction Kit	Qiagen

Material	Supplier
QIAGEN Miniprep Kit	Qiagen
QIAGEN® Plasmid Mega Kit	
QIAquick Gel Extraction Kit	
QIAquick PCR Purification Kit	
Ammonium Persulfate	Sigma-Aldrich
Bis-acrylamide	
Bradford reagent	
Albumin from Bovine Serum	
Dulbecco's Modified Eagle Medium	
Fetal Bovine Serum	
Glacial Acetic Acid	
Glycine, for electrophoresis	
Hanks' Balanced Salt solution	
Kanamycin	
L-arabinose	
Lysogeny Broth	
Methanol	
Sodium Chloride	
Penicillin-Streptomycin	
Sodium Dodecyl Sulfate	
SOC medium	
Sodium Hydroxide	
TEMED	
Terrific Broth	
Tris base	
Trypsine	
TWEEN-20	

Material	Supplier
MN511/MN512 minicircle system	System Biosciences
ZYCY10P3S2T <i>E. coli</i>	
5x Sample Buffer	Thermo Scientific
Lane Marker Reducing Sample Buffer	
Pierce ECL Plus Western Blotting Substrate	
SYBR®Safe DNA Gel Stain	

B. Chemical-Competent Cells Preparation

1. Inoculate empty cells into 5 mL LB, 37 °C, O/N (8-12 h).
2. Take 1 mL O/N culture to inoculate 50 mL LB at 37 °C.
3. OD wanted 0.4-0.5, which takes about 1h~2h.
4. Decant the culture to pre-cooled 50 mL tube, place on ice for 10 minutes to cool culture until 0 °C.
5. Centrifuge at 5000 rpm, for 10 minutes.
6. Pour the supernatant, put the tube bottom up for 10-20 s to let the liquid residues out.
7. Re-suspend cells with 30 mL pre-cooled 0.1 mol/L CaCl₂·2H₂O for every 50mL culture (Just shake, not pipetted).
8. Centrifuge at 5000 rpm, for 10 minutes.
9. Pour the supernatant, put the tube bottom up for 10-20 s to let the liquid residues out.
10. Re-suspend cells with 2 mL pre-cooled 0.1 mol/L CaCl₂·2H₂O for every 50 mL culture.
11. Add 1.2 mL 50% glycerol into 2 mL solution & aliquot to EP tube (each 50 µL).
12. Cells snap open with liquid nitrogen & stored at -80 °C.

C. Chemical Transformation

1. Put the prepared frozen chemical-competent ZYCY10P3S2T *E. coli* cells (as

Appendix II-B shown) on ice to thaw.

2. Add ~200 ng plasmid solution into the 50 μ L cells.
3. Flick to mix plasmids and cells.
4. Incubate the mixture on ice for 30 min.
5. Heat shock the cells at 42 °C for 30 s (no shaking).
6. Put back on ice immediately for 2 min.
7. Add 250 μ L pre-warmed SOC medium.
8. Seal lids; Recover the culture at 37 °C for 1h by shaking in the incubator.
9. Spread 20-200 μ L culture on plate with Kanamycin, incubate in 37 °C, O/N.

D. Lipofectamine® 2000 Reagent Protocol (96-well plate)

Component	96-well
Adherent cells	1 x 10 ⁴
Opti-MEM® Medium	25 μ L x 4
Lipofectamine® 2000 Reagent	1, 1.5, 2, 2.5 μ L
Opti-MEM® Medium	125 μ L
DNA (0.5-5 μ g/ μ L)	2.5 μ g
Diluted DNA Total	25 μ L
Diluted Lipofectamine® 2000 Reagent	25 μ L
DNA-lipid complex per well	10 μ L
Final DNA used per well	100 ng
Final Lipofectamine® 2000 Reagent used per well	0.2-0.5 μ L

1. Seed cells to be 70-90% confluent at transfection.
2. Dilute four amounts of Lipofectamine® Reagent in Opti-MEM® Medium.
3. Dilute DNA in Opti-MEM® Medium.
4. Add diluted DNA to diluted Lipofectamine® 2000 Reagent (1:1 ratio).
5. Incubate for 5 minutes at room temperature.

6. Add DNA-lipid complex to cells.
7. Incubate cells for 2 days at 37°C. Then analyse transfected cells.

E. Xfect™ Transfection Reagent Protocol (6-well plate)

1. Prepare cells for transfection: For adherent cells: One day prior to the transfection, plate cells in 1 mL of complete growth medium so that the cells will be 50–70% confluent at the time of transfection.
2. Thoroughly vortex Xfect™ Polymer.
3. In a microcentrifuge tube, dilute 5 µg of your plasmid DNA with Xfect™ Reaction Buffer to a final volume of 100 µL. Mix well by vortexing for 5 sec at high speed.
4. Add 1.5 µL Xfect™ Polymer to the diluted plasmid DNA. Mix well by vortexing for 10 sec at high speed.
5. Incubate for 10 min at room temperature to allow nanoparticle complexes to form.
6. Spin down for 1 sec to collect the contents at the bottom of the tube.
7. Add the entire 100 µL of nanoparticle complex solution dropwise to the cell culture medium. Rock the plate gently back and forth to mix.
8. Incubate the plate at 37°C for 4 hr.
9. Remove nanoparticle complexes from cells by aspiration, replace with 2 mL fresh complete growth medium, and return the plate to the 37°C incubator until time of analysis. Peak expression is typically reached 48 hr post-transfection.

F. T4 DNA Ligase Application Protocol

1. Assemble the following reaction in a sterile microcentrifuge tube.

a) For the ligation of MN512 vector and COL7A1 gene,

Mass ratio vector: insert = 2:1

MN512	200 ng
COL7A1	100 ng
Buffer(10×)	1 μL
Ligase enzyme	0.5 μL
Nuclease-Free Water to final volume	10 μL

b) For the ligation of MN512C7 vector and COL7A1 promoter (TSP),

Molar ratio vector: insert=1:1

$$\frac{\text{ng of vector} \times 1.19(\text{insert})}{15.6(\text{vector})} \times \frac{10}{1} = \text{ng of insert}$$

MN511M18Col7(no CMV)	800 ng
TSP	610 ng
Buffer(10×)	3 μL
Ligase enzyme	0.5 μL
Nuclease-Free Water to final volume	30 μL

2. Incubate the reaction at 16 °C for 12 hours.

3. Denature the ligase at 70 °C for 10 minutes.

G. Protein Quantification

1. Prepare BSA standard protein 0.1-1.4 mg/mL (0.1, 0.5, 1.0, 1.4 mg/mL, respectively).

2 mg/mL BSA: 1 mg (0.001 g)→500 μL PBS

mg/mL	0.1	0.5	1.0	1.4
2 mg/mL BSA	10 μL	50 μL	100 μL	140 μL
PBS	190 μL	150 μL	100 μL	60 μL

2. Add 5 μL /well in 96-well plates, including buffer only (blank), standards and samples, using 3 parallel wells for each sample.
3. Gently mix Bradford reagent in the bottle and bring to room temperature.
4. Add 250 μL Bradford for each well, mix on a shaker for 30 seconds
5. Incubate at R/T for 5-45 min
6. Measure absorbance at 595 nm, within 60 min.

H. Flow Cytometry Analysis

Sample preparation

1. Trypsinize cells from well, centrifuge at 1200 rpm for 5 min.
2. Discard supernatant, wash pellet, re-suspend in 5 mL medium.
3. Take out 500 μL in an Eppendorf tube.
4. Centrifuge at 1200 rpm for 5 min.
5. Discard supernatant, wash with 5% FBS in Hanks' Balanced Salt solution (HBSS) once.
6. Re-suspend in 1 mL HBSS with 5% FBS.
7. Drop 2 drops of Propidium Iodide in each 1 mL sample, incubate 30 min at room temperature.
8. Filter through 50 μm filter.
9. Load sample to flow cytometer.

Flow cytometry gating

The analysed cells were screened through a few gates to eliminate those gritty particles, conjugated cells, or dead cells. Exciting light is 488 nm. FL1 is 530/30 filter; FL2 is 585/40 filter; FL3 is 670LP.

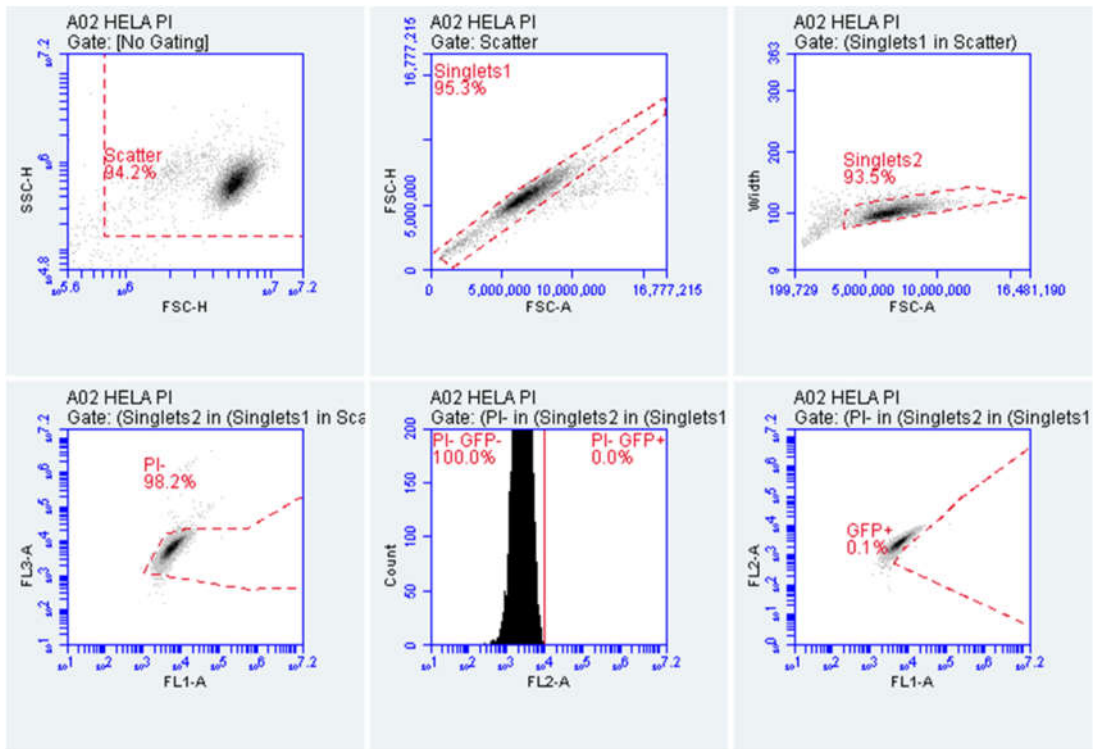


Figure vi. Gating results of the non-transfected HeLa cells (negative control).

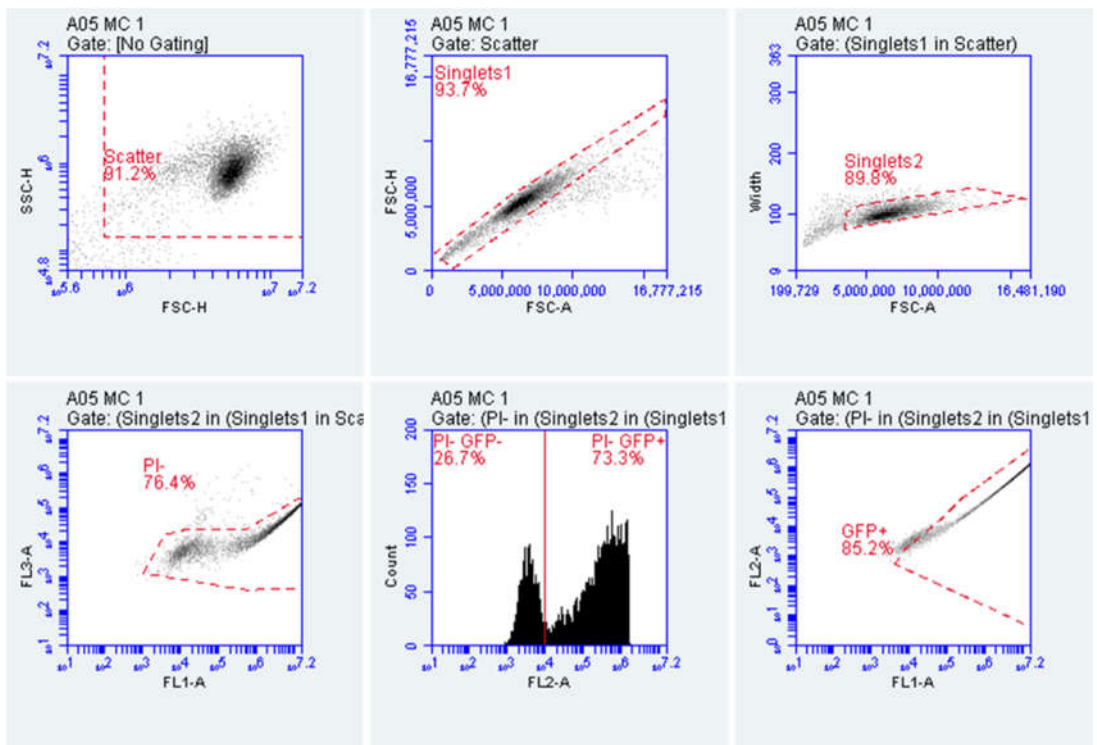


Figure vii. Gating results of the minicircle transfected HeLa cells.

I. DNA Electrophoresis

TAE Buffer: 4.84 g Tris Base

1.14 mL Glacial Acetic Acid

2 mL 0.5M EDTA (pH 8.0)

Bring the total volume up to 1 L with water

Add Tris base to ~900 mL H₂O. Add acetic acid and EDTA to solution and mix.

Pour mixture into 1 L graduated cylinder and add H₂O to a total volume of 1 L.

Preparing the agarose gel:

1. Weigh 0.8 g Agarose powder and add it to a 100 mL TAE Buffer
2. Heat the agarose in a microwave until the solution becomes clear.
3. Add 10 μ L of SYBR[®]Safe DNA stain when solution has cooled to ~ 40 °C
4. Place the combs in the gel casting cassette.
5. Pour the melted agarose solution into the cassette and let it congealed.
6. Place the gel in the electrophoresis chamber.
7. Add TAE Buffer until there is about 2-3 mm of buffer over the gel.

Loading and running the gel

1. Add 5 μ L of 6X Sample Loading Buffer to each 25 μ L sample
2. Record the order each sample will be loaded on the gel, controls and ladder.
3. Carefully pipette 20 μ L of each sample/Sample Loading Buffer mixture into separate wells in the gel.
4. Pipette 10 μ L of the DNA ladder standard into at least one well
5. Connect the positive electrode to the positive inlet (red) and negative electrode to the negative inlet (black).
6. Run the gel at 80V for 30-45 minutes depending the size of the DNA
7. Visualize the bands under short wave bypass on G-Box.

J. Western Blotting for Type VII Collagen Detection*Reagents preparation*

1.5M Tris pH 8.8: (500mL) Tris 90.855 g

1M Tris pH 6.8: (500mL) Tris 60.57 g

10% SDS: (200mL) SDS 20 g

10% APS: (10mL) APS 1 g

2*sample buffer: (10 mL)

1M Tris pH 6.8 1 mL

10% SDS 4 mL

Glycerol 2 mL

β -mercaptoethanol 1 mL

Bromophenol blue 20 mg

10*running buffer: (1 L)

SDS 10 g

Tris 30.3 g

Glycine 144.1 g

Transfer buffer: (1 L)

10* running buffer 100 mL

H₂O 700 mL

Methanol 200 mL

Transfer buffer = running buffer+20% methanol

10*TBS: (500 mL)

Tris 12.1 g

NaCl 40 g

→ pH 7.6

TBST: (500 mL)

10* TBS 50 mL

H₂O 450 mL

Tween 20 0.5 mL

Sample preparation

Because type VII collagen is secreted protein, supernatant is harvested 3 days post

changing medium. The harvested supernatant is concentrated through Amicon® Ultra-15 Centrifugal Filter Units, until the volume is within 2 mL. The concentrated samples were quantified by Bradford reagent method as Appendix II-G shown.

Bis-acrylamide Gel preparation

Running gel	6%	Stacking gel	3%
Volume	5 mL	Volume	2 mL
dH2O	2.6 mL	dH2O	1.5 mL
30% Bis-Acrylamide	1.0 mL	30% Bis-Acrylamide	0.2 mL
1.5M Tris pH 8.8	1.3 mL	1.0M Tris pH 6.8	0.25 mL
10% SDS	0.05 mL	10% SDS	0.02 mL
10% APS	0.05 mL	10% APS	0.02 mL
TEMED	4 µL	TEMED	2 µL

Denature samples: 98 °C for 10 min.

SDS-PAGE: 100V 15min + 130V 70min

Transfer: 80V 1h

Blocking: 5% BSA in TBST, 1h, 37 °C

Primary antibody:

Collagen type VII antibody (1:2500*2, 1:4000*2) in blocking buffer, O/N, 4 °C

Wash with TBST for 4*5min

Secondary antibody:

Anti-rabbit HRP 1:5000 in blocking buffer, 1h, R/T

Wash with TBST for 4*5min

Use Pierce ECL Plus Western Blotting Substrate Thermo® #32134(25mL kit)

Mix luminol: H₂O₂ = 40:1